The Antioxidant Activity of Recombinant Rat Fatty Acid Binding Protein 1 T94A Variant

by

Tyson Le

A Thesis submitted to the Faculty of Graduate Studies

In Partial Fulfillment of the Requirements for the degree of

MASTER OF SCIENCE

College of Pharmacy

Rady Faculty of Health Sciences

University of Manitoba

Winnipeg, Manitoba

Copyright © 2017 by Tyson Le

Table of Contents

Abstract

Liver fatty acid binding protein (FABP1) is present at high levels in the liver and functions as an antioxidant. A single nucleotide polymorphism was found resulting in the FABP1 T94A variant. Currently, it is not known how this mutation affects the antioxidant activity of FABP1 T94A. Rat cDNA within pGEX-6p-2 vector was isolated from bacterial cells and the mutation was induced using site-directed mutagenesis. The plasmid was transformed into competent cells that were cultured and used for the expression of FABP1 T94A. The protein was purified using the GST affinity tag system and its antioxidant capacity was assessed using DCF fluorescence assay. FABP1 T94A showed that the mutation did not change the protein's ability to scavenge hydroxyl radicals. Thiobarbituric Acid Reactive Substances Assay was used to determine the FABP1 T94A's antioxidant activity in simulated hydrophilic and lipophilic environments induced by the azo compounds AAPH and MeO-AMVN. T94A was able to act as an antioxidant in both cases performing almost equivalent to FABP1. However, when bound with fatty acids (palmitate and alpha-bromo palmitate) the ability of T94A as an antioxidant may be affected. In conclusion, The T94A variation of FABP1 does not have a loss of function in regards to acting as an antioxidant but the extent of function may be influenced by ligand binding.

Acknowledgements

I would like to thank my advisor Dr. Frank J Burczynski for his guidance throughout my Master program. His patience and advice was insurmountable and was essential for helping me grow not only as a student but as an individual. His excellent insight and passion for science gave me so much support and encouragement. I am forever grateful for what he has done and I am very lucky to have such an amazing mentor.

My sincere thanks to both Dr. Yuewen Gong and Dr. Ted M Lakowski for their extraordinary help with troubleshooting experimental procedures. I learned a lot from their extensive knowledge and their passion in science is inspiring. I am grateful to Dr. Neal M Davies for giving me the opportunity to join this research lab. Your generosity and support have enriched my life significantly.

I would like to thank fellow students Samaa Alrushaid, Refaat Omar, Yannick Traoré, Ryan Lillico, Andy Chen, Joshua Fang, Jiaqi Yang, and Nick Stesco. They not only helped my studies as a graduate student but also made the journey very enjoyable.

I appreciate the College of Pharmacy at the University of Manitoba for the financial support for my graduate studies.

Finally, special thanks to my parents, Tai Le and Huong Nguyen, and my brother, Thomas Le for their endless encouragement and support.

List of Figures

List Tables

Abbreviations

°C	Degree Celsius
%	Percent
µg	Microgram
µL	Microliter
µM	Micromolar
AAPH	2,2'-Azobis(2-methylpropionamidine) dihydrochloride
ADH	Alcohol dehydrogenase
ALD	Alcoholic liver disease
ALDH	Acetaldehyde dehydrogenase
BSA	Bovine serum albumin
BMI	Body mass index
bp	base pairs
cDNA	Complementary DNA
CRABP	Cellular retinoic acid binding proteins
CRBP	Cellular retinol-binding protein
CVD	Cardiovascular disease
CYP2E1	Cytochrome P450 2E1
DCF	Dichlorofluorescein
DCFH	2, 7-dichlorodihydrofluorescein
DCFH-DA	2, 7-dichlorofluorescein-diacetate
DNA	Deoxyribonuclieic acid

DTT	dithiothreitol
ECM	Extracellular matrix
E.coli	*Escherichia coli*
EDTA	Ethylene diaminetetracetic acid
FA	Fatty acids
FABP1	Liver fatty acid binding protein
FABPs	Fatty acid binding proteins
FATP5	Fatty acid transport protein 5
FF	Fastflow
FFA	Free fatty acid
FPLC	Fast protein liquid chromatography
GI	Gastrointestinal
GPx	Glutathione peroxidase
GSH	Glutathione
HCl	Hydrochloric acid
HCC	Hepatocellular carcinoma
H_2O	Water
H_2O_2	hydrogen peroxide
HPLC	High-performance liquid chromatography
HSC	Hepatic stellate cell
I-BABP	Intestinal bile acid-binding protein
IPTG	Isopropyl b-D thiogalactoside
kDa	Kilo Daltons

L	Liters
LB	Luria-Bertani
LCFA	Long chain fatty acids
LDL	Low-density lipoprotein
MALDI-TOF	Matrix Assisted Laser Desorption Ionization Time-of-Flight
NaCl	Sodium chloride
MDA	Malondialdehyde
OD	Optical density
MeO-AMVN	and 2,2'-Azobis(4-methoxy-2,4-dimethylvaleronitrile)
Met	Methionine
MetSO	Methionine sulfoxide
Min	Minutes
mL	Milliliters
mM	Milimolar
MSR	Methionine sulfoxide reductase
MSRox	Methionine sulfoxide reductase oxidized
NADPH	Nicotinamide adenine dinucleotide
NAFLD	Non-alcoholic fatty liver disease
NAPQ1	N-acetyl-p-benzoquinone-imine
NASH	Nonalcoholic steatohepatitis
O2•	Superoxide anion radical

OH•	Hydroxyl radical
PA	Palmitate
PBS	Phosphate buffered saline
PCR	Polymerase chain reaction
PMSF	phenylmethylsulfonyl fluoride
PPARα	Peroxisome proliferator activated receptor alpha
PPRE	Peroxisome proliferator response element
ROO•	Peroxide
ROS	Reactive oxygen species
rpm	Revolutions per minute
RT	Room temperature
SDS-PAGE	Sodium Dodecyl Sulfate Polyacrylamide Gel Electrophoresis
SNP	Single nucleotide polymorphism
SOD	Superoxide dismutase
T2DM	Type-2 diabetes mellitus
TAG	Triacylglycerol
TBARS	Thiobarbituric Acid Reactive Substances
TBS	Tris buffered saline
TE	Tris-EDTA
TEMED	N,N,N',N-tetramethylethylenediamine
TBST	Tris buffered saline with Tween 20
TG	Triglyceride
ThR	Thioredoxin reductase

TNF-α	Tumor necrosis factor alpha
UV	Ultraviolet
V	Volts
α-Br-PA	Alpha-bromo-palmitate

Chapter 1: Introduction

Liver: Structure and Function

The liver is considered to be the largest internal organ in the human body weighing approximately 1.5 kg in an adult. It is situated predominantly in the upper right quadrant of the abdominal cavity, protected by the ribcage and connects to the diaphragm. A peritoneal fold connects the liver to both the diaphragm and the abdominal wall, while the falciform ligament divides the liver into left and right lobes (Boyer *et al.,* 2012). The caudate and quadrate lobes make up the right lobe, inferiorly and posteriorly respectively. The source of the liver's venous blood is supplied mainly by the gastrointestinal (GI) tract from the portal vein and from the systemic circulation by the hepatic artery. This dual blood supply from the portal vein and the hepatic artery gives the liver a unique structural organization that makes the liver a prime metabolic organ and allows for greater than 2000 L of blood to flow through the organ daily. Nutrient-rich blood originating from the GI tract enters the liver using the portal vein. The hepatic artery, portal vein and the bile duct create the portal triad. Hepatic sinusoids are supplied with blood by portal venules and hepatic arterioles forming a lattice of vessels in the liver. This vasculature enables the liver to release metabolic products from hepatocytes into the blood and remove macromolecules from the blood. Hepatocytes compose up to 60 % of the total cell population of the liver and approximately 78 % of the liver volume (Gershwin *et al.,* 2012). These cells perform functions the liver is known for, such as the homeostasis of glucose, synthesis of bile acids from cholesterol, protein synthesis, and the metabolism of drugs and toxins.

Most drugs are metabolised in the liver where xenobiotic compounds undergo biotransformation reactions. There are two phases in the biotransformation reaction, phase I and phase II. In phase I, the parental compound is converted to a metabolite that is water soluble by cytochrome P450. In phase II the drug metabolite is conjugated to small sized molecules in the body such as acetate and glucuronides to increase water solubility and elimination. Cytochrome P450 are enzymes that are located in the endoplasmic reticulum's membrane and are found mostly in the liver. The bio-activation of xenobiotics by these enzymes may generate electrophiles or free radicals that could result in oxidative stress that harms the cells. An example of this is seen in the overdose of acetaminophen. Acetaminophen is converted to an intermediate that is highly electrophilic, N-acetyl-p-benzoquinone-imine (NAPQ1) by cytochrome P450. Normally glutathione in the body can counteract this intermediate, however, glutathiones become depleted during an overdose. NAPQ1 can then form adducts with proteins leading to oxidative stress (Stirnimann *et al.,* 2010). Diclofenac is another drug whose intermediates undergo redox cycling and can result to oxidative stress (Boelsterli 2003). Metabolised in the liver, Diclofenac undergoes ring hydroxylation, a reaction catalyzed by cytochrome P450, hCYP2C9. This produces the metabolite 4'-hydroxydiclofenac (Stierlin and Faigle, 1979). The intermediate 4'-hydroxydiclofenac can be oxidised further to a p-benzoquinone imine, a electrophile that is involved with redox cycling and is able to generate oxidative stress (Tang *et al.,*1999). Drug metabolites can have adverse effects on cells as some of these intermediates increase free radicals resulting in oxidative stress.

Oxidative Stress in the Liver

A cellular state where there is an imbalance between free radical production and antioxidant defenses that favours free radical production, is called oxidative stress. Reactive oxygen species (ROS) can haphazardly react with organic molecules. ROS are molecules with a partial reduction to their oxygen with some species containing an unpaired electron making them unstable and highly reactive (Figure 1 and Table 1). Some examples of ROS include the peroxide ($ROO^{\bullet}$), the superoxide anion radical ($O_2^{\bullet}$) and the hydroxyl radical ($OH^{\bullet}$). They have the ability to react with biological molecules such as nucleic acids, lipids, and proteins leading to problems causing disorder and potentially the destruction of cells. Such problems include the inactivation of enzymes, destruction of membranes, degradation of lipids, and modifications to DNA causing mutations. Normally hepatocytes produce small amounts of ROS that are controlled by antioxidant defenses (Kobayashi *et al*., 2013). However, in a diseased liver there would be an overabundance of ROS from overproduction or the impairment of antioxidant defenses. A small quantity of electrons leak to oxygen in the mitochondrial respiratory chain reactions producing a ROS, the superoxide anion (Schlezinger *et al*., 2006). ROS can also be generated in the cell by reactions through the exposure of chemicals, radiation, pesticide hormones, and pollution; reactions by cytochrome P450 to detoxify xenobiotics; enzymes such as cyclooxygenase, xanthine oxidase, and lipoxygenase; and NADPH oxidation system. Normally ROS produced in cells are usually in low to moderate levels that can actually serve several functions. Such roles of ROS include cellular signalling pathways; mitogenic response initiation; and protection against bacteria, fungi, and viruses.

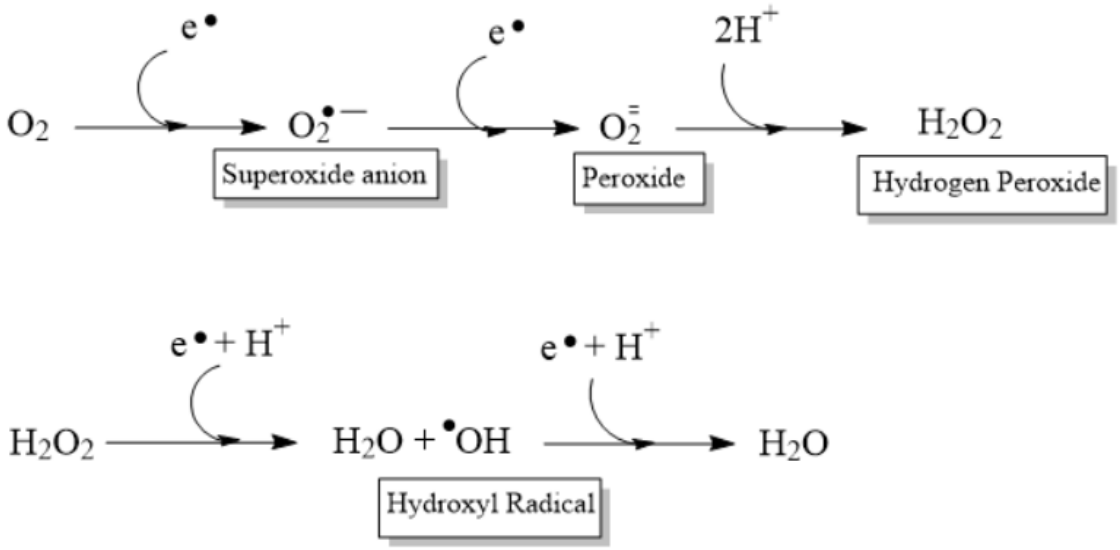

Figure 1: Production of ROS. ROS are formed as intermediate products when molecular oxygen is converted to water.

Table 1: ROS sources and description

ROS	Description	Source
O2•, Superoxide anion	A reduced state of O2 by accepting an electron. Generated by the electron transport chain and autoxidation.	Mitochondria NADPH Oxidase Xanthine Oxidase Cyclooxygenase 5-lipoxygenase
OH•, Hydroxyl radical	Despite being short lived the molecule will attack any biological element as it is exceptionally reactive.	Super Oxide Dismutase Peroxisomes
H_2O_2, Hydrogen peroxide	Two electron reduced oxygen. Forms by reduction of O2 or the dismutation of O2•. Are able to pass though membranes since they are lipid soluble.	Fenton Reaction Haber-Weiss Reaction

Lipid Peroxidation

Unsaturated lipids are susceptible to attack by free radicals, especially polyunsaturated fatty acids due to the exposed methylene groups on carbons. The methylene groups are more vulnerable because the double bonds between the carbons make the hydrogens more reactive. The reaction will cause lipid degradation by oxidation, which is termed lipid peroxidation. Lipid peroxidation contains a chain of reactions with three stages: initiation, propagation, and termination as shown in Figure 2. In the initiation step, a polyunsaturated fatty acids' hydrogen is attacked by a free radical forming a lipid radical. The next stage, propagation, produces a lipid peroxyl radical when the lipid radical reacts with oxygen. The lipid peroxyl radical can undergo several reactions; attack membrane components (ie. proteins and lipids), continue propagation by attacking a hydrogen from an adjacent fatty acid side chain, or react with one another terminating the reaction. The termination of lipid peroxidation occurs when lipid peroxyl radicals react with each other or when the lipid peroxyl radicals are neutralized by antioxidants. Lipid peroxidation produces aldehydes such as 4-oxo-2-nonenal, 4-hydroxy-2-nonenal, and the most prevalent malondialdehyde (MDA). DNA adducts are formed through lipid peroxidation that causes DNA mutagenesis. Lipid peroxidation also results in the destruction of the membrane structure and function by the degradation of polyunsaturated fatty acids (Zhang *et al*., 2006). The membrane may be perturbed by lipid hydroperoxides trying to migrate to the surface resulting in the reduction of membrane fluidity, inactivation of bound receptors and enzymes, damage to integrity, and increase in permeability (Pamplona 2008). Albano *et al.* (2005) reported that peroxide products are related to the development of fibrosis from non-alcoholic fatty liver disease (NAFLD).

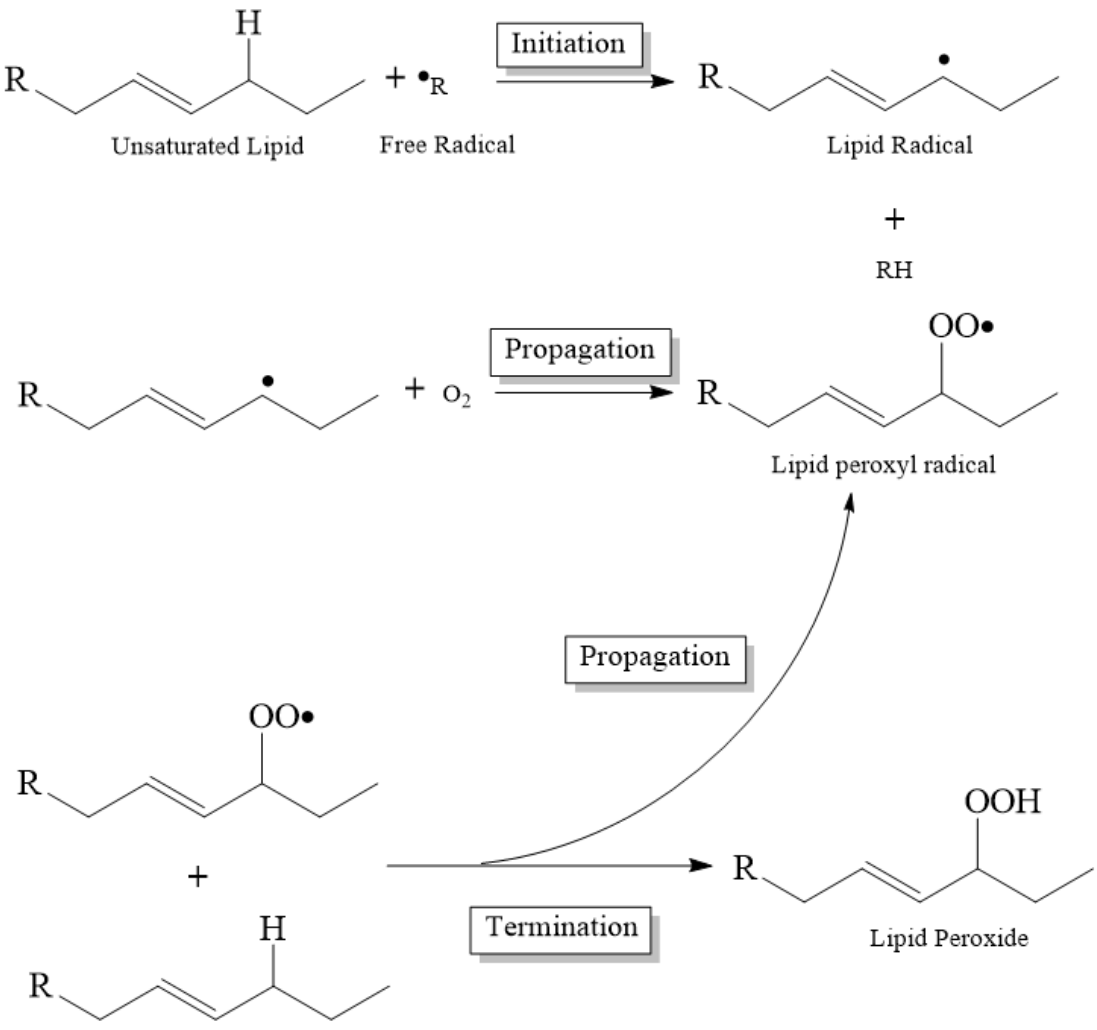

Figure 2: The process of lipid peroxidation. In the initiation step, an unsaturated lipid is attacked by a OH• producing a lipid radical. This lipid radical reacts with oxygen resulting in a peroxyl radical. The peroxyl radical can either combine with one another or attack nearby fatty acid side chains producing another peroxyl radical and a lipid peroxide (propagation).

The study measured concentrations of antibodies against lipid peroxidation products: MDA, oxidised cardiolipin, and arachidonic acid hydroperoxides in 167 NAFLD patients. They reported that the antibodies against these lipid peroxidation products were significantly higher in patients with NAFLD than in the controls. Konishi *et al.* (2006) found that increased amounts of lipid peroxidation products are involved in the development of chronic hepatitis C. The study investigated the levels of a lipid peroxidation product, 8-isoprostane, in 75 patients with chronic hepatitis C. Using an enzyme immune assay, the study reported elevated levels of 8-isoprostane in the plasma of patients with chronic hepatitis C compared to the controls.

Oxidation of Protein

Protein oxidation occurs when a protein is covalently altered by via ROS or secondary by-products of lipid peroxidation such as MDA. The oxidation of proteins can modify them by cleaving peptides with free radicals, reacting with lipid peroxidation products forming protein cross-links, and changing the structure of amino acids. Examples of these modifications include tyrosine crosslinks, amino acid interconversions, and the formation of protein carbonyls (Stadtman and Levine, 2000). One method to measure protein oxidation caused by ROS is to look at these protein-bound carbonyls. In determining oxidized protein, the protein can be reacted with 2, 4-dinitrophenylhydrazine where the products of the derivatization reaction is detected by enzyme-linked immnosorbent assay (Buss *et al*., 1997), spectrophotometer, or by high-performance liquid chromatography (HPLC) (Weber *et al*., 2015). Ultraviolet (UV) light and xenobiotics are examples of exogenous sources accountable for the oxidation of proteins while electron transport chain and cytochrome P450 enzymes are endogenous sources. Cysteine and methionine side chains are the most vulnerable to an attack by ROS, however, all amino acid

residues are susceptible. Table 2 lists some examples of oxidation products when amino acid are oxidized. Protein fragmentation and cross-linkages are a result of oxidation of the protein backbone and amino acid side chains (Kowalik-Jankowska *et al*., 2006). The function of a protein may be disrupted if oxidative damage occurs at the active sites. Protein oxidation will influence enzyme activity, proteolysis, and signal transduction (Lobo *et al.,* 2010). The oxidation of proteins have been found to be involved in the pathogenesis of many diseases. Such diseases include liver disease (Cichoż-Lach and Michalak, 2014), end stage renal disease (Drüeke *et al*., 2002), aging (Liochev 2005), Alzheimer's disease (Huang *et al*., 2016), and cardiovascular disease (He and Zuo, 2015).

Table 2: Amino acids and their respective oxidation products

Amino Acids	Oxidation Products
L- Arginine	Glutamic semialdehyde
L- Cysteine	Cysteic acid, cysteine sulfenic acid
L- Histidine	Aspartic acid, asparagines
L- Lysine	Aminoadipic semialdehyde
L- Methionine	Methionine sulfoxide, methionine sulfone
L- Tryptophan	4-Hydroxytryptophan, nitro-tryptophan
L- Tyrosine	p-Hydroxyphenylacetaldehyde

Oxidation of DNA

DNA mutagenesis is a consequence of DNA oxidation (Lee *et al*., 2002). Mutations that can initiate cancer and cell death (senescence) are caused by oxidative damage of DNA ranging from erroneous replication, transcription, and translation. Cancers, some forms of liver disease, and aging are linked to DNA oxidation. DNA can be damaged at the sugar-phosphate backbone or the base. DNA bases can undergo opening, hydroxylation, contraction, and ring saturation when hydroxyl radicals react with the base (Xu *et al.*, 1999). ROS can react with DNA to form adducts which are the most common type of damage to DNA. MDA, a product of lipid peroxidation reacts with DNA to form DNA adducts (Warnakulasuriya *et al.*, 2008). Deoxyadenosine, deoxycytidine, and deoxyguanosine adducts are products between DNA bases (A, C, and G respectively) and MDA (Marnett 2000). Another lipid peroxidation product, 4-hydroxy-2-nonenal, generate DNA adducts when it reacts with DNA. 4-hydroxy-2-nonenal target DNA bases' nitrogen atoms forming ethno-DNA-base adducts. Some examples of these adducts are N2, 3-ethenodeoxyguanosine, N4-ethenodeoxycytidine, and ethenodeoxyadenosine with DNA bases G, C, and A respectively (Loureiro *et al*., 2000).

Oxidative stress in Mitochondria

The mitochondria is most vulnerable to oxidative stress as this organelle produces ROS as undesirable products due to its function in energy metabolism. ROS can alter the membrane of the mitochondria affecting its permeability. Mitochondrion DNA and ribosomes can be attacked by ROS resulting in impaired or loss of protein synthesis (Bailey and Cunningham, 2002). In alcoholic liver disease (ALD), elevated levels of ROS are released in liver mitochondria. The oxidative stress within the organelle is related to inflammation in ALD. In NAFLD the

mitochondria is damaged by ROS leading to changes in protein synthesis, decreasing the expression of genes involved with beta-oxidation. Additionally, lipid peroxidation products can increase the permeability of the mitochondria and inactivate the mitochondrion respiratory chain (Videla 2009).

Liver Diseases Related to Oxidative Stress

When discussing liver diseases, substance abuse with drugs or alcohol must be discussed. The process of inflammation and fibrosis, which can ultimately result in cirrhosis and hepatocellular carcinoma (HCC), occurs in chronic liver disease. There are many types of liver diseases caused by numerous aspects and one of these factors is oxidative stress. Considered part of the pathogenesis of various liver diseases, oxidative stress is related to diseases such as alcoholic liver disease (ALD), viral hepatitis, non-alcoholic steatohepatitis, and hemochromatosis (Feng *et al.*, 2011; Singal *et al.*, 2011). Small quantities of ROS are produced in the liver that are usually inactivated by a complex antioxidant system. This system is responsible for maintaining redox homeostasis in mammals. Unfortunately this is not the case in chronic liver diseases where there are excessive ROS overwhelming the antioxidant system. This disturbs the homeostatic balance between antioxidants and oxidants causing oxidative stress (Li *et al.*, 2014). Oxidative stress is an outcome of several chronic liver diseases and is also involved in liver fibrosis and remodeling (Parola and Robino, 2001). Oxidative stress plays a role in pathways regulating protein expression, hepatic stellate cell (HSC) activation, and gene transcription. Within the liver, parenchymal cells are most often exposed to oxidative stress. Furthermore, endothelial cells, Kupffer cells, and HSC are the most sensitive to oxidative stress.

ROS is responsible for endothelial cell dysfunction by increasing leukocyte adhesion and vascular endothelial permeability (Szocs 2004).

Fibrosis is characterized by liver scarring as a response to liver injury. Hepatitis B and C virus, alcohol consumption, and cholestasis can lead to liver fibrosis. HSC plays a major role in liver fibrosis, where HSC overproduces the extracellular matrix (ECM) when the liver is injured. Cirrhosis is a resultant of the advancement of liver fibrosis. ROS from damaged hepatocytes can activate HSC. Activated hepatic stellate cells transform into their myofibroblast-like phenotype that are responsible for producing the extracellular matrix. ROS can activate the redox intracellular pathway in HSC that can allow them to transform and increase the production of collagen (Brenner *et al.,* 2012). Cytokines such as tumor necrosis factor alpha (TNF-α) are produced by Kupffer cells during oxidative stress; these cytokines increase apoptosis and inflammation of the cell.

ALD is a common cause of global mortality and morbidity. ALD results from excessive alcohol consumption and encompasses a spectrum that includes hepatic steatosis, hepatitis, fibrosis, cirrhosis, and in extreme cases can lead to HCC. Oxidative stress and inflammation occur in the liver of patients with alcohol abuse. The overproduction of ROS and oxidative stress within liver cells are related to liver damage from alcohol (Cederbaum *et al.,* 2009). Alcohol dehydrogenase (ADH) oxidizes ethanol into acetaldehyde, which is then metabolized into acetate by acetaldehyde dehydrogenase (ALDH) in the mitochondria. Cytochrome P450 2E1 (CYP2E1) can also oxidize ethanol. CYP2E1 has a significant role in the degradation of ethanol during excessive consumption of alcohol. Oxidative stress and cell death result when there is a release of ROS originating from the activation by CYP2E1. Another method of ethanol degradation occurs in peroxisomes by catalase, however, this rarely occurs during alcohol metabolism and

occurs during a fasted state (Handler and Thurman, 1990). Catalase utilizes hydrogen peroxide to oxidize ethanol. Between the three pathways (ADH, cytochrome P450, and catalase) to metabolize ethanol, the pathways using ADH and CYP2E1 produces large amounts of NADH or $NADP^+$ that increase the number of ROS.

One of the most widespread chronic liver disease is NAFLD. Steatosis, nonalcoholic steatohepatitis (NASH) and cirrhosis are a part of the band of disorders that NAFLD covers. Unwarranted fat is accumulated in the liver due to the disruption in the oxidation, transport, uptake, and synthesis of fatty acids describes the pathogenesis of NAFLD. The increase occurrence and main risk factor for NAFLD is obesity (Sattar *et al.,* 2014). Liver damage from NAFLD is facilitated by oxidative stress and the renin-angiotensin system (Morris *et al.,* 2013). Angiotensin II is a pro-oxidant, can increases fibrosis and has pro-inflammatory effects in the liver. Elevated levels of angiotensin II have a significant effect on ROS production within the liver (Wei *et al.,* 2008). In NAFLD, oxidative stress is caused by an increase in the expression of mitochondrial CYP2E1 (Kathirvel *et al.,* 2010). Disruption of mitochondrial function further contributes to the oxidative stress as increased rates of mitochondrial β-oxidation from the accumulated fatty acids (FA) will increase the amount of ROS generated by the electron transport chain (Gusdon *et* al., 2014).

Antioxidants

Substances present in low concentrations that have the ability to thwart or interrupt its oxidation are termed antioxidants (Halliwell 1990). Oxidative stress occurs when there is an imbalance between free radicals and antioxidants. In this state, there is an excessive production of ROS compared to their elimination and there is a decrease in the number of antioxidants.

Under normal conditions, the body contains both enzymatic and non-enzymatic antioxidants that have a critical role in the management of oxidative stress. Some examples of antioxidant enzymes are superoxide dismutase (SOD), catalase, and glutathione peroxidase (GPx). While glutathione (GSH), ascorbic acid, and vitamin E are examples of non-enzymatic antioxidants. Table 3 shows some enzymatic and non-enzymatic antioxidants. The livers' antioxidant defense system's essential constituents are SOD, GPx, GSH, and catalase. SOD catalyzes the reaction between two superoxide radicals producing hydrogen peroxide and oxygen. Found in the mitochondrial matrix is the SOD that uses magnesium in its active site while the copper-zinc SOD are reside in the intermembrane space of the mitochondria and cytosol. Co-factors GSH and nicotinamide adenine dinucleotide (NADPH) as well as enzymes glutathione reductase and glutathione peroxidase make up the glutathione peroxidase system. The co-factor GSH is a thiol that is synthesized in cytosol in its reduced form. GSH acts as an antioxidant as well as a detoxifying co-substrate for enzymes such as peroxidases and glutathione reductase. From the cytosol, GSH can be translocated to the mitochondria and nucleus. GPx are a group of selenium-containing enzymes found within the cytoplasm that detoxifies lipid peroxides and hydrogen peroxides by oxidizing them with GSH. Catalase are mostly found in peroxisomes but are also present in the mitochondria.

Table 3: List of antioxidants

Antioxidant	Description
SOD	Catalyzes the dismutation of superoxide anion, found all mammalian cells
α-tocopherol	Scavenges oxidant agents in hydrophobic
Glutathione	Considered to be the most important non-enzymatic antioxidant
Ascorbic acid	Scavenge ROS produced by cellular metabolism
Glutathione peroxidase	Catalyze the elimination of organic peroxides and hydrogen peroxide
Albumin	Thiol groups scavenge ROS and sulphydryl groups can react with H_2O_2 and peroxyl radicals

Catalase functions to catalyze the decomposition of hydrogen peroxide thus producing water and oxygen. Since oxidative stress has a crucial role in liver diseases, it is logical to utilize antioxidants as a therapeutic strategy to mediate these disorders.

Fatty Acid Binding Protein Family

Fatty acid binding proteins (FABPs) can be found in both vertebrates and invertebrates. Vertebrate FABPs can be subdivided into four categories (Subfamily I-IV) based on the similarity in amino acid sequence and binding specificity (Hanhoff *et al.,* 2002). In the first subfamily FABPs are further categorized into cellular retinoic acid binding proteins (CRABP-I and II) and cellular retinol-binding protein (CRBP-I, II, III, and IV). Subfamily II consists of the liver fatty acid binding protein (FABP1) and intestinal bile acid-binding protein (I-BABP). Both of these proteins share a similar sequence and can bind to larger ligands such as eicosanoids and bile acids due to their large binding site. Subfamily III only comprises I-FABP and subfamily IV contains adipocyte, brain, epidermal, heart, myelin, and testis fatty acid binding protein.

Found in ample quantities in the cytoplasm, FABPs are responsible for the translocation, uptake, and metabolism of cellular long-chain fatty acids (LCFA). FABPs can bind to many lipophilic ligands such as LCFA, bile acids, and retinoids (Veerkamp and Maatman, 1995). The transport of these ligands is done in several steps: (1) the ligand binds to the outer leaflet of the plasma membrane-adsorption; (2) ligand crosses the membrane- membrane transport proteins such as fatty acid transport protein can help facilitate hydrophobic ligands pass through; and (3) the ligand leaves the plasma membrane on the cytosolic leaflet- desorption. FABPs can increase the rate of dissociation of the ligands from the plasma membrane by increasing the ligands

aqueous solubility (Vork *et al.,* 1993) or increase the ligands transfer to membranes by a diffusive process or by direct interaction (Thumser and Storch, 2000).

Ligands bind to FABPs with different affinity, selectivity, and mechanism (Chmurzynska 2006). This is due to small structural differences caused by the deviations of the FABPs amino acid sequences. Despite the small structural differences between FABPs, the 3-dimensional fold is maintained in all types of FABPs. The protein fold is a β-barrel fold that is generated when 10 anti-parallel β-strands form a β-sheet structure (Banaszak *et al.,* 1994). The fold is described as "β-clam" by (Sacchettini *et al.,* 1988) due to possessing a clamshell like appearance.

Liver Fatty Acid Binding Protein

In 1969, two fractions found in rat liver were discovered having the ability of binding bilirubin and bromosulfophthalein (Levi *et al.,* 1969). The one with the lower molecular mass was termed Z protein. This Z protein was found in the cytosol of the liver, small intestine, and kidneys (Ockner *et al.,* 1972). Furthermore, the Z protein had a molecular weight of approximately 14 kDa and was able to bind LCFA. Due to the protein's ability to bind to LCFA it was named liver fatty acid binding protein or fatty acid binding protein 1 (FABP1).

FABP1 Gene

Rat FABP1 gene is on chromosome 4 with a length of 3.78 kb in the q33 region (Sweetser *et al.,* 1987). Whereas, the human FABP1 gene is located in the p12 region and is 5.07 kb in length on the second chromosome (Chen *et al.,* 1986). Both of these FABP1 genes have four exons interrupted by three introns. Rat and human FABP1 are 89.8% similar (Betts and Russell, 2003) and they share significant protein secondary structures, two α-helices and 10 β-

sheets (Sharma and Sharma, 2011; Cai *et al*., 2012). Figure 3 illustrates the amino acid sequence alignment between rat and human FABP1. It was determined that peroxisome proliferator response element (PPRE) has a significant role in the regulation of FABP1 (Veerkamp and Maatman, 1995). PPRE is located in the promoter region of FABP1 and is activated by peroxisome proliferator activated receptor alpha (PPARα) (Schachtrup *et al*., 2004).

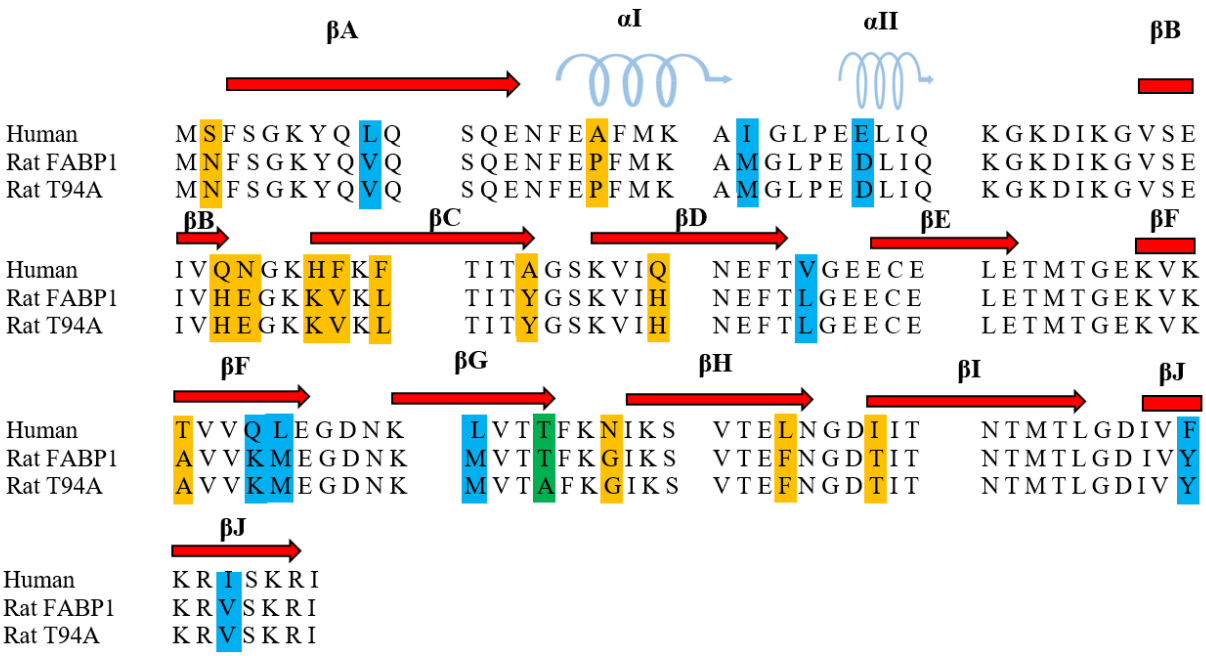

Figure 3: Amino acid sequence alignment of rat and human FABP1s. Conservative amino acid substitutions are shown in the orange while in blue shows the nonconservative substitutions. Protein secondary structures are indicated above the sequence where spirals are α-helices αI and αII and arrows are β-sheets βA- βJ.

FABP1 Structure

The binding cavity of FABP1 can be described as "clam" shaped due to the protein's tertiary structure composed of two antiparallel 5-stranded sheets that are 90° to each other, this is similar to the other members of the FABP family (Banaszak *et al.,* 1994). The two α-helices form a "lid" of the binding cavity acting as a portal controlling the entry and exit of ligands (Thompson *et al.,* 1997). The ligand binding cavity of FABP1 is the largest of the fatty acid binding protein (FABP) family. The size of the binding pock*et* allows the protein to bind to more than two ligands. This peculiar ability makes FABP1 the most unique in the FABP family (Thompson *et al.,* 1997). FABP1's structure has alternating hydrophobic and hydrophilic domains as revealed through computer aided predictions (Takahashi *et al.,* 1983). With this pattern, FABP1 has a hydrophilic surface that allows the protein to be solubilized in the aqueous cytoplasm. Furthermore, the hydrophobic domain allows the protein to bind to various ligands (Veerkamp *et* al., 1990). There are two binding sites in the binding pocket with a high and low affinity (Rolf *et al.,* 1995). When FABP1 binds to a LCFA, the ligand's carboxyl faces inside the binding cavity at the higher affinity site. In contrast, the carboxyl faces away from the binding cavity at the weak affinity site (He *et al.,* 2007). Since both the high and low affinity binding sites form hydrophobic interactions they are interdependent. The structure of FABP1 is illustrated in Figure 4.

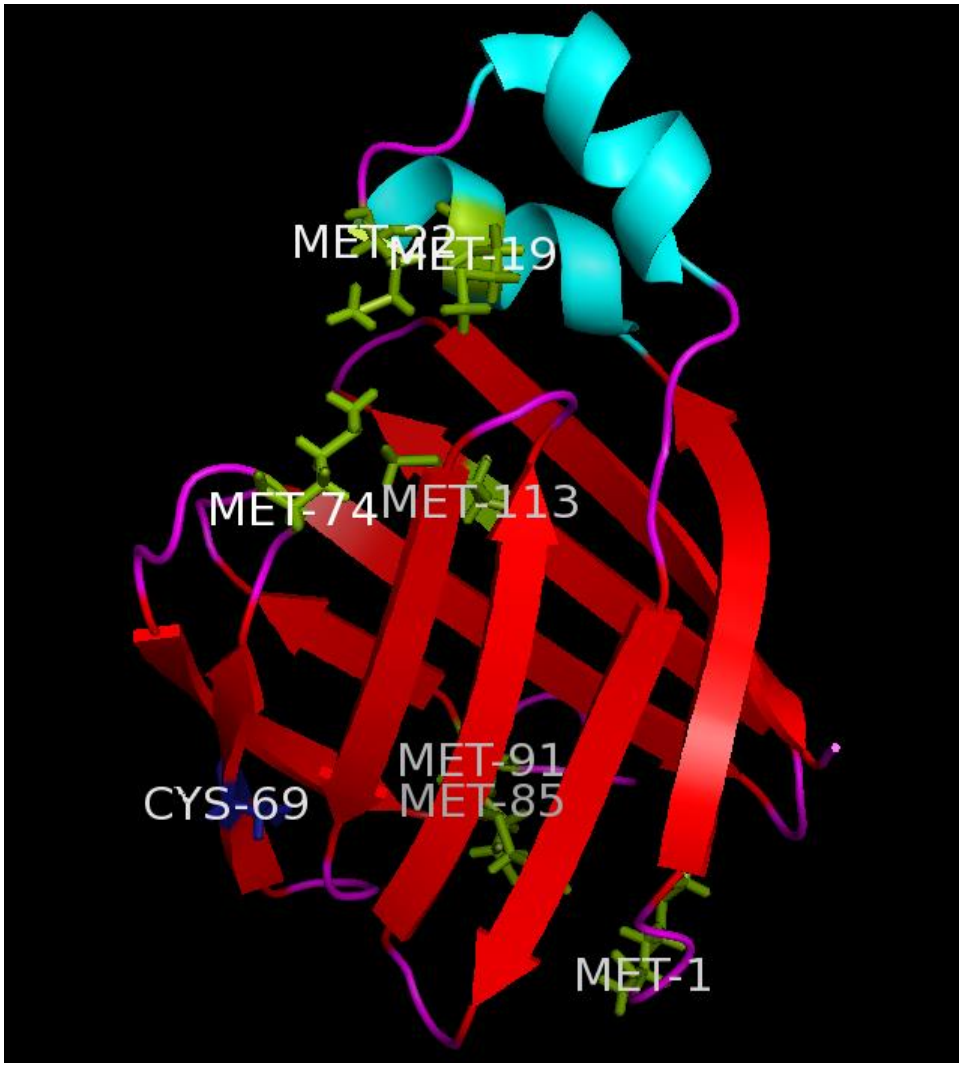

Figure 4: The structure of FABP1. Structure shows the 2 α-helices in turquoise and 10 β-sheets in red. Figure generated using PyMOL.

FABP1 Function

FABP1 functions as fatty acid chaperones where they actively transport fatty acids to other areas of the cell. FABP1 can bind LCFA and its oxidation products, eicosanoids (Furuhashi and Hotamisligil, 2008), bile acids (Favretto *et al*., 2015), hypolipidemic agents like PPARα agonists (Rolf *et al.,* 1995), peroxisome proliferators, bilirubin, bile acids, selenium, heme, and other hydrophobic ligands. FABP1 has various functional roles as indicated by the broad ligands that bind to its binding site (Coe and Bernlohr, 1998). FABP1 can transport fatty acids to the endoplasmic reticulum for cell signalling, trafficking, and membrane synthesis (Furuhashi and Hotamisligil, 2008). Fatty acids can also be transported by FABP1 to peroxisomes or mitochondria for oxidation, storage in lipid droplets, and nucleus to activate genes involved with fatty acids. When FABP1 transports its ligands to the nucleus, it targets the bound ligands to PPARα where the activation of genes transcribing LCFA transport, metabolism, and uptake takes place (Wolfrum *et al.,* 2001). By transporting PPARα agonists, FABP1 is part of the signal transduction pathway of PPARα (Huang *et al.,* 2002). The transcriptional rate of FABP1 gene is increased by PPARα agonists which would increase FABP1 mRNA and protein levels (Nakagawa *et al.,* 1994). It has been reported that the increase in FABP1 correlates with peroxisomal fatty acid oxidation and FABP1 levels (Kawashima *et al.,* 1983). Consequently, FABP1 can be targeted for therapeutics due to their relations with nuclear receptor activities. FABP1 has roles ranging from the intracellular transport and storage of fatty acids, fatty acid acyl-CoA esters, to LCFA metabolism and compartmentalization (Bass 1988). In a sense, FABP1 is analogous to serum albumin being the intracellular equivalent (Wang *et al.,* 2015). Albumin has thiol and sulphydryl groups to scavenge or react with ROS giving the protein antioxidant capabilities. This antioxidant ability is also seen with FABP1.

Several studies on FABP1 have shown that the protein can act as a potent cellular antioxidant (Wang *et al.,* 2005; Yan *et al.,* 2009). Wang *et al.* (2005) had Chang cells derived from human liver tissue without FABP1 expression transfected with a constructed plasmid that contained human FABP1 gene. Hydrogen peroxide and hypoxia were then used to put these cells under oxidative stress. ROS levels were increased in the non-transfected Chang cells causing cellular apoptosis (Wang *et al.,* 2005). The study reported that cells transfected with FABP1 cDNA had a reduction in ROS levels illustrating that FABP1 might have a role in the inhibition of cellular apoptosis caused by ROS and can act as a cytoprotectant during oxidative stress. It was also shown that FABP1 decreased the activity of caspase-1, thus reducing apoptosis in the transfected cell line.

Since methionine and cysteine residues are more sensitive to oxidation (Stadtman *et al.,* 2003) it was suggested that these amino acid groups play a key role in FABP1's antioxidant function. Cysteine group and methionine residues were identified in FABP1 where they can participate in S-thiolation/dethiolation reactions and cellular ROS scavengers, respectively (Thomas *et al.,* 1995; Odani *et al.,* 2000). Expressed greatly in the liver, methionine sulfoxide reductase (Moskovitz *et al.,* 1996) can reduce FABP1's methionines back after being oxidized by ROS into sulfoxides (Levine *et al.,* 1999). The cyclic reactions of FABP1 methionine residues and methionine sulfoxide reductase illustrates FABP1's antioxidative ability (Figure 5).

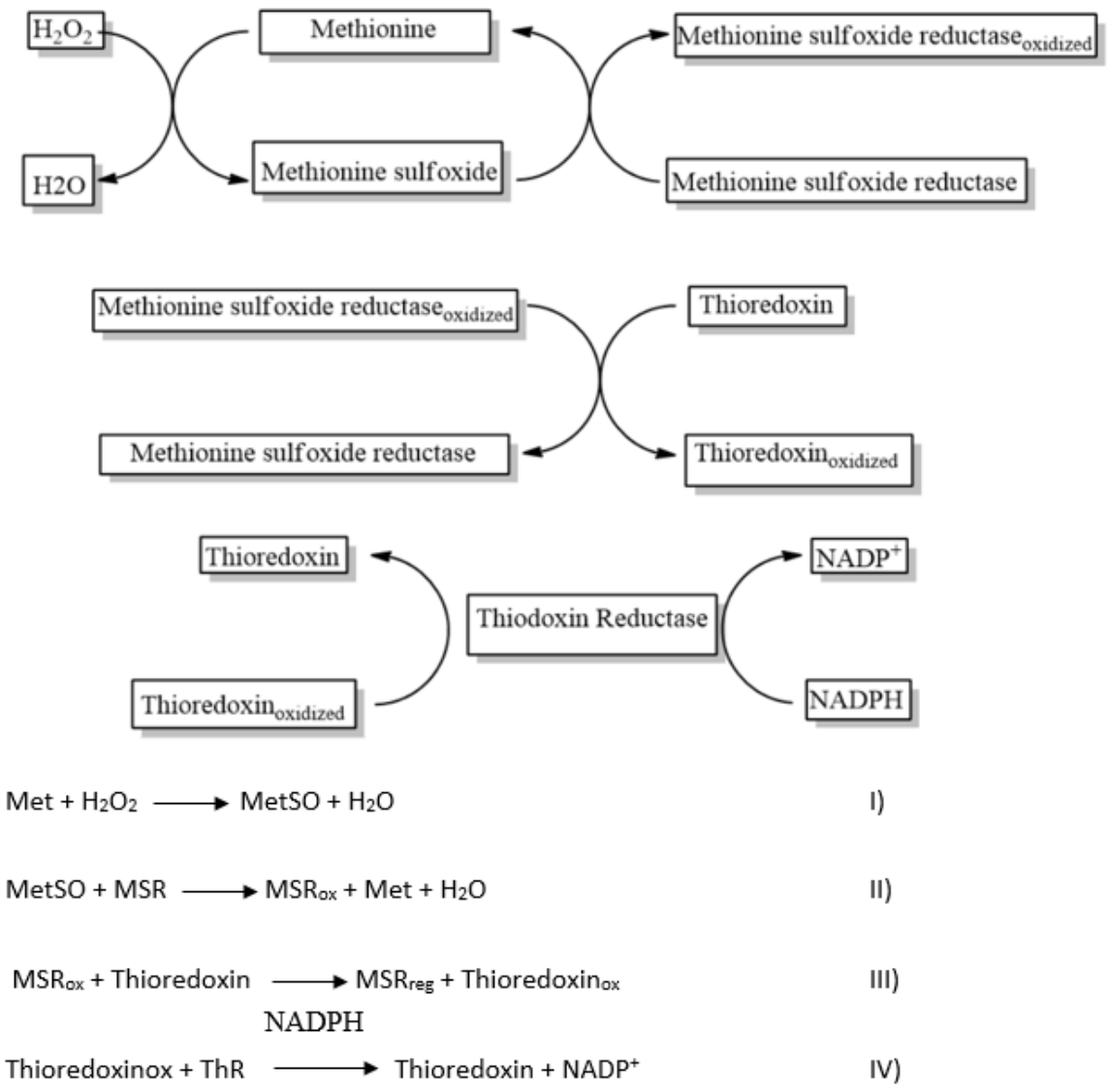

Figure 5: The oxidation and reduction of methionine residues (Met) catalyzed by methionine sulfoxide reductase (MSR). I) A methionine residue is oxidized by hydrogen peroxide resulting in methionine sulfoxide (MetSO) and water. II) The MetSO is reduced by MSR producing the oxidized protein (MSRox), water and the methionine residue. III) The oxidized MSR is reduced back by thioredoxin. (IV) Thioredoxin which is now oxidized can be reduced by thioredoxin reductase (ThR) with NADPH acting as an electron donor.

Yan *et al*. (2009) reported that FABP1's antioxidant ability was due to methionine residues found at amino acids 1, 19, 22, 74, 85, 91, and 113. Using Matrix Assisted Laser Desorption Ionization Time-of-Flight (MALDI-TOF) mass spectrometry the group found that methionine groups are mainly responsible for the antioxidant function of FABP1. In a hydrophilic environment, five out of the seven methionine groups were oxidized. Furthermore, in the lipophilic environment three of the seven methionine groups were available for oxidation. The group reported that FABP1's methionine groups at position 1 and 113 are most prone to oxidation by ROS. Their study also suggested the FABP1 has greater protection to oxidative stress within the cytosol as antioxidative activity was greater when free radicals were generated by a hydrophilic domain than a lipophilic domain. Furthermore, another study done by Yan *et al.* (2010) demonstrated diminished FABP1 expression with FABP1 siRNA resulting in increased ROS levels after oxidative stress generated by hydrogen peroxide. High hepatic oxidative stress was also reported during chronic ethanol ingestion in FABP1 gene knock out mice (Smathers *et al.,* 2003) and suggests that FABP1's antioxidant activity may be crucial in the pathogenesis of ALD. There are various sources elucidating the antioxidative potency of FABP1 consequently, this protein may be an avenue for novel treatment of liver diseases.

FABP1 T94A Mutation

The FABP1 T94A mutation is a variant of the wild type FABP1 that has a single nucleotide polymorphism (SNP) at the 94^{th} position. The mutation substitutes a polar, moderate sized threonine with a non-polar, small sized alanine residue. The mutation is considered to be common having a minor allele frequency of 26-38%. The SNP occurs within the N-terminus of the protein which makes up a portion of a fatty acid binding site (Gao *et al.,* 2010). The

substitution may have some critical consequences on FABP1's function since the SNP is conserved in different species such as *Mus Musculus* and *Rattus Norvegicus*. Brouillette *et al.* (2004) sought to determine if the FABP1 T94A variant would influence the plasma lipoprotein levels of patients treated with fenofibrate and in their fasting state. The sequence analysis revealed this SNP of FABP1 in exon 3. The study screened 130 French-Canadians and found that carriers of the A94 allele have higher triacylglycerol (TAG) levels after being treated with fenofibrate (Brouillette *et al.,* 2004). These results conflicted with their expectation of lower TAG levels in the mutant suggesting an impaired function. They reported that the T94A carriers had elevated levels of plasma free fatty acids (FFA) and also possessed lower body mass index (BMI) and waist size than the homozygotes. Robitaille *et al.* (2004) reported when FABP1 T94A mutant carriers consume a diet rich in fat they were protected against high apo B levels while the homozygotes display higher apo B levels. Another study confirmed this trend that reported European female carriers having increased serum levels of fasting TAG and low-density lipoprotein (LDL) (Fisher *et al.,* 2007). In contrast with these results, male carriers in China had higher body weights, BMI, and plasma TAG levels (Tian *et al.,* 2015). Although the studies above do not clearly demonstrate the functionality of the FABP1 T94A mutant they do suggest the T94A variant's impact on fatty acid trafficking.

Gao *et al.* (2010) reported the FABP1 T94A mutant was associated with decreased amounts of fatty acid uptake and hence loss of function. The study transfected mutated FABP1 into Chang cells and found FABP1 T94A to have a reduced ability to transport fatty acids, which resulted in a decrease in cholesterol production and fatty acid re-esterification of triglycerides. Martin *et al.* (2014) and Huang *et al.*(2014) looked at ligand specificity, structure, and mode of ligand binding of the FABP1 T94A variant with PPARα agonists and LCFA, respectively. Using

circular dichroism, Martin *et al.* (2014) found that the variant is significantly different from the wild type FABP1 in its secondary structure, thermal stability, and structural response to fenofibric acid. When the mutant FABP1 T94A was expressed in primary human hepatocytes there was a diminished transcription of proteins such as PPARα, FABP1, and fatty acid transport protein 5 (FATP5). Thus, Martin *et al.* (2014) determined that the mutation weakens the induction of PPARα transcriptional activity. With these findings, Martin *et al.* (2014) demonstrated that the FABP1 T94A variant does not display a loss of function but rather a change in function. Huang *et al.* (2014) determined that the variant was resistant to urea denaturation, had little to no changes to its specificity and affinity to fatty acids, experienced less prominent changes in structure when bound to LCFA, secondary structure was significantly altered when bound to triglyceride synthesis intermediates, and finally had a weaker influence on PPARα-regulated protein transcription compared to the normal FABP1. Additionally, Huang *et al.* (2015) determined that the FABP1 T94A variant has a higher binding affinity to cholesterol than the wild type. The variant also had faster high-density lipoprotein and low-density lipoprotein mediated NBD-cholesterol uptake. Studies have been done to gain insight on the impact of the FABP1 T94A mutant, however, it's influence is still not clear specifically the mutant protein's function. An area that has not been investigated is whether the FABP1 T94A mutant's antioxidant activity is altered.

Hypothesis and Objective

Hypothesis

Studies completed in our laboratory demonstrated that FABP1 can act as a novel endogenous hepatic antioxidant (Wang *et al.,* 2005; Yan *et al.,* 2009). It was determined that the methionine residues are responsible for the antioxidant function. While there are studies attempting to elucidate the effect of the FABP1 T94 mutant, the variant's antioxidant activity has yet to be evaluated. Specifically, it is unknown whether the folding of the mutant protein would make methionine groups available to react with ROS. In the present studies, the null hypothesis to be tested is that the FABP1 T94A variant does not alter the antioxidant activity compared to the normal FABP1. The results of Martin *et al.* (2014) and Huang *et al.* (2014) indicate that while there are differences in secondary structure between FABP1 and the variant there was no abolishment or alteration to the binding of ligands. Hence, the folding of the FABP1 mutant may not conceal the methionine groups responsible for FABP1's antioxidant activity.

Objective

The objectives of this study was to mutate recombinant rat FABP1 to the T94A variant using site-directed mutagenesis and to investigate the protein's antioxidant activity.

Chapter 2: Materials and Methods

Materials

Chemicals used in this thesis were purchased from Sigma-Aldrich (St. Louis, Missouri, USA) if not stated otherwise.

Methods

Plasmid DNA Purification

Bacterial stock from a previous study (Yan *et al*., 2009) was checked to ensure it contained the pGEX-6P-2 plasmid vector with FABP1 cDNA. To do this, the plasmid was isolated from cells and purification of plasmid DNA was achieved using the Plasmid Mini Kit (QIAGEN, Montreal, Canada) based on the methods of Birnboim and Doly (1973). Bacteria from glycerol stocks were streaked on LB agar with ampicillin (100 µg/ml) and were incubated at 37°C overnight (16 hours). Single colonies were selected the next day and cultured in 3 mL of Luria-Bertani Broth (LB) Lennox (ThermoFisher Scientific, Mississauga, Canada) with 100 µg/ml of ampicillin in 15 mL tubes and shaken using a MaxQ 5000 (ThermoFisher Scientific, Mississauga, Canada) at 200 rpm and 37°C overnight. Bacterial cells were harvested by pelleting the samples at 6000 g at 4°C for 15 min using a Sorvall LYNX 4000 Centrifuge (ThermoFisher Scientific, Mississauga, Canada) and the F14-14x50cy rotor.

Following centrifugation the supernatant was removed and pellet resuspended with 0.3 mL Buffer P1 with RNase A (one vial of RNase A was added to Buffer P1 to a final concentration of 100 µg/ml before use) by gently pipetting up and down until a smooth homogenate was obtained (no clumps). Samples were transferred to 1.5 mL Eppendorf tubes

adding 0.3 mL of Buffer P2. Lysates were inverted 4-6 times and incubated at room temperature (RT) for 5 minutes (min). Pre-chilled Buffer P3 was added (0.3 mL) to the lysates and mixed by inverting 4-6 times. Samples were then incubated on ice for 5 minutes then centrifuged at 13,600 g in a single speed Micro-centrifuge Model 235B (ThermoFisher Scientific, Mississauga, Canada) for 10 minutes at 4°C (cold-room). While samples were being centrifuged, the Qiagen tips were equilibrated with 1 mL Buffer QBT and allowed the column to empty by gravity flow. The supernatant of the lysate was added to the tips that were washed twice after the samples have completely flowed through with 2 mL Buffer QC. The DNA was eluted with 0.8 mL Buffer QF into clean 1.5 mL Eppendorf tubes and then precipitated by 0.7 volumes (0.56 mL per 0.8 mL of eluted volume) of RT isopropanol. Eluted DNA was briefly vortexed and centrifuged at 13,600 g for 30 minutes at 4°C. The supernatant was carefully decanted to avoid disturbing the glassy pellet. The DNA pellet was then washed with 1 mL 70% ethanol and centrifuged at 13,600 g for 10 minutes at RT. The pellet was air dried for 10 minutes and dissolved with 50 µL TE buffer (10 mM Tris, 1 mM EDTA, pH 8.0). Plasmid DNA yield was determined using the Nanodrop 2000 and samples stored at -20°C.

Restriction Enzyme Digestion

With the plasmid purified, confirmation on its identity was required in determining whether the restriction enzyme digestion was performed successfully. Restriction enzyme mapping uses enzymes that recognize specific sequences and accurately cleaves sites adjacent to the recognized sequences. Yan *et al*. (2009) used BamHI and XhoI recognition sites to ligate the FABP1 cDNA into the p-6GEX-6P-2 plasmid vector. The isolated plasmid was cleaved with BamH1 and XhoI (Roche Diagnostics, Indianapolis, USA) for the mapping. Table 4 illustrates

the components for the restriction enzyme reaction. Plasmid DNA concentration was adjusted to a final concentration of 1 µg/µL, where 10 µL was mixed by gently pipetting up and down in a tube containing double distilled water, and 10 x restriction enzyme buffer. Finally, the restriction enzymes were added, solution mixed gently pipetting and followed by brief centrifugation using a Mandel Mini Centrifuge (Mandel Scientific, Ontario, Canada). The reaction mixture was incubated in a water bath at 37°C for 4 hours. Products of the restriction enzyme digestion were analyzed using agarose gel electrophoresis.

Agarose Gel Electrophoresis

To analyze the digests from the restriction enzyme mapping, the DNA fragments must be separated. A simple technique to separate DNA fragments based on size is agarose gel electrophoresis. The restriction enzyme digests would cleave the plasmid DNA vector from the cDNA FABP1, which can be visualized on an agarose gel where their sizes can be compared to a standard DNA ladder. A 1.0% agarose gel was made by dissolving 1.0 g agarose (Amresco, Solon, USA) in 100 mL 1X TBE buffer (89 mM Tris pH 7.6, 89 mM boric acid, 2 mM EDTA) by heating the solution for 2 minutes with a microwave oven (GoldStar Waveplus II MS-71TC, operating frequency 2450 MHz; Maximum output 700 W) in a 250 mL Erlenmeyer flask. Once the flask was cool to touch (1 min), 5 µL of SYBR Safe DNA Gel Stain (ThermoFisher Scientific, Mississauga, Canada) was swirled into the solution. The solution was poured into a pre-chilled gel casting platform (Bio-Rad, Hercules, USA) with the sample comb inserted and sealed with tape. Bubbles were removed with a needle or an Eppendorf tip and the gel was left at RT until it solidified.

Table 4: Constituents in the restriction enzyme reaction

Reagent	Volume (µL)
Double distilled water	7
Restriction Enzyme Buffer (10x)	2
DNA (1 µg/µL)	10
BamHI	0.5
XhoI	0.5

The seal was removed and the gel inside the casting platform was placed into the electrophoresis tank followed by filling the tank with approximately 800 mL 1X TBE buffer. To prepare the samples, 5 µL of DNA sample or 2 µL DNA ladder with 2 µL loading buffer (20% Ficoll 400, 0.1 M Na_2EDTA pH 8.0, 1.0% SDS, 0.25% bromophenol blue) were added pipetting up and down. The comb was removed and samples with dye loaded into the wells. Following sample loading, 5 µL of SYBR Safe was added to each side of the tank. The gel ran at 100 V for 90 minutes and was visualized with a UV transilluminator from Alpha Innotech FluorChem FC2 MultiImage If.

Site-Directed Mutagenesis

The introduction of a mutation to the pGEX-6P-2 vector containing the rat FABP1 cDNA (Figure 6) was done using the GENEART Site-Directed Mutagenesis System (Invitrogen, ThermoFisher Scientific, Mississauga, Canada). This kit is a simple and efficient way to generate site-directed mutants. Site-directed mutagenesis is a technique that allows the precise introduction and control of the nucleotide base substitutions, deletions, or additions. By mutating cDNAs one can study the translated product for engineering new and existing proteins or investigate their biological functions (Trehan *et al.,* 2016). The latter purpose allows researchers to model mutations that exist in the human population and examine their relevance to diseases at a molecular level (Carter 1986).

This technique is based on polymerase chain reaction and requires mutagenic primers, DNA templates, polymerase, nuclease, and host cells. While there are many kits for site-directed mutagenesis some characteristics remain similar. The basic steps of site-directed mutagenesis are methylation, mutagenesis reaction, and transformation for selection as shown in the workflow in

Figure 7. Forward and reverse primers used in site-directed mutagenesis are complementary with one another and with the template but with the desired mutation at the centre thus, called mutagenic primers. When designing mutagenic primers nucleotides should be 30-45 base pairs (bp) long not including the mutation and have a guanine and cytosine content around 40%. These primers should be completely complementary to each other with no extended ends. Furthermore, there should not be any palindromic sequences to prevent secondary structures from forming. The mutagenic primers in this study, shown in Figure 8, were designed using the GeneArt Primer and Construct Design Tool.

In the same way as PCR, site-directed mutagenesis uses high-fidelity polymerases to extend the mutagenic primers that result in nicked PCR products that re-circularizes forming doubly-nicked plasmids. The GENEART Site-Directed Mutagenesis System combines the methylation and mutagenesis reaction in one step. The reaction mixture is displayed in Table 5. The methylated plasmid then undergoes mutagenesis within a thermal cycler with the settings listed in Table 6 creating multiple copies of mutagenic plasmids. To increase the mutagenesis efficiency and colony yield an *in vitro* recombination was done. The recombination reaction components are listed in Table 7. The reaction was vortexed and incubated at RT for 10 minutes. The reaction was stopped by adding 1 µL of 0.5 M EDTA, mixed well, and placed on

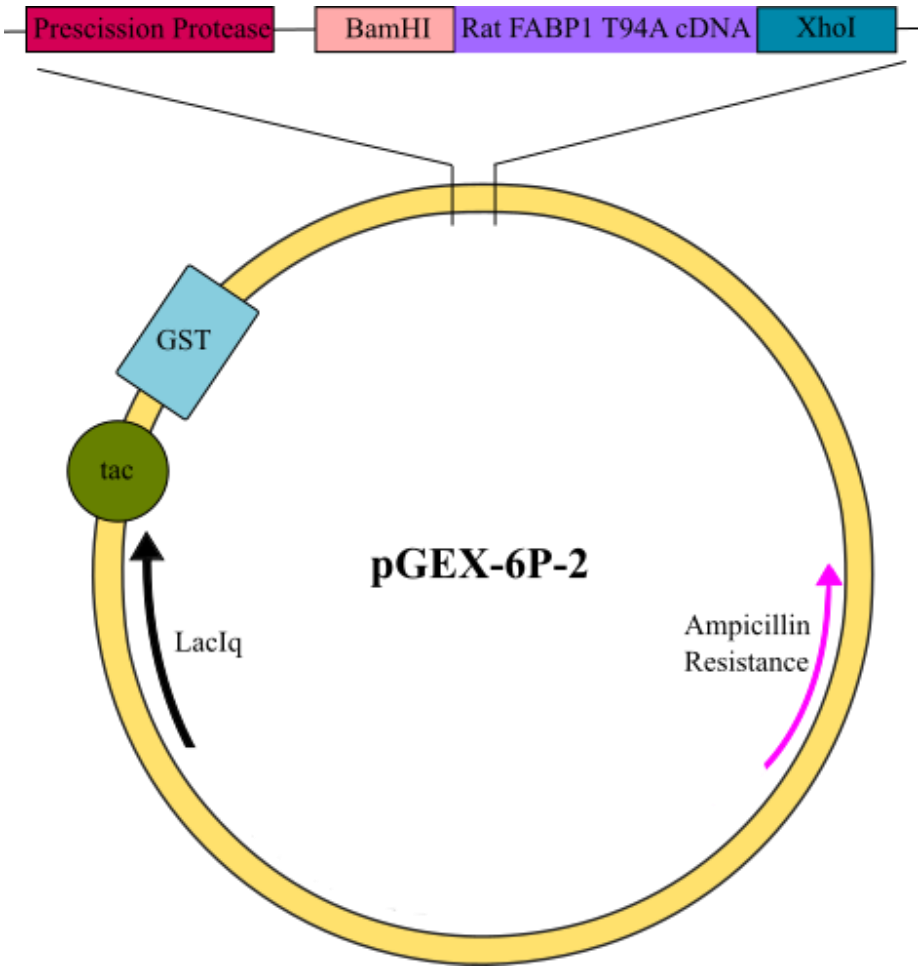

Figure 6: Illustration of the pGEX-6P-2 vector containing rat FABP1 cDNA. The pGEX-6P-2 is a glutathione S-transferase (GST) fusion vector. The vector possess a GST tag giving a way to purify the fusion protein. This vector contains a PreScission Protease sequence that allows for the cleavage of the fusion protein into the FABP1 protein and the GST tag. The sequence sites for BamHI and XhoI restriction enzymes enable the insertion of the rat FABP1 cDNA. Furthermore, the vector contains sequences for LacIq and antibiotic resistance gene against ampicillin used for protein expression with isopropyl b-D thiogalactoside (IPTG) and selection of bacteria with the appropriate vector, respectively.

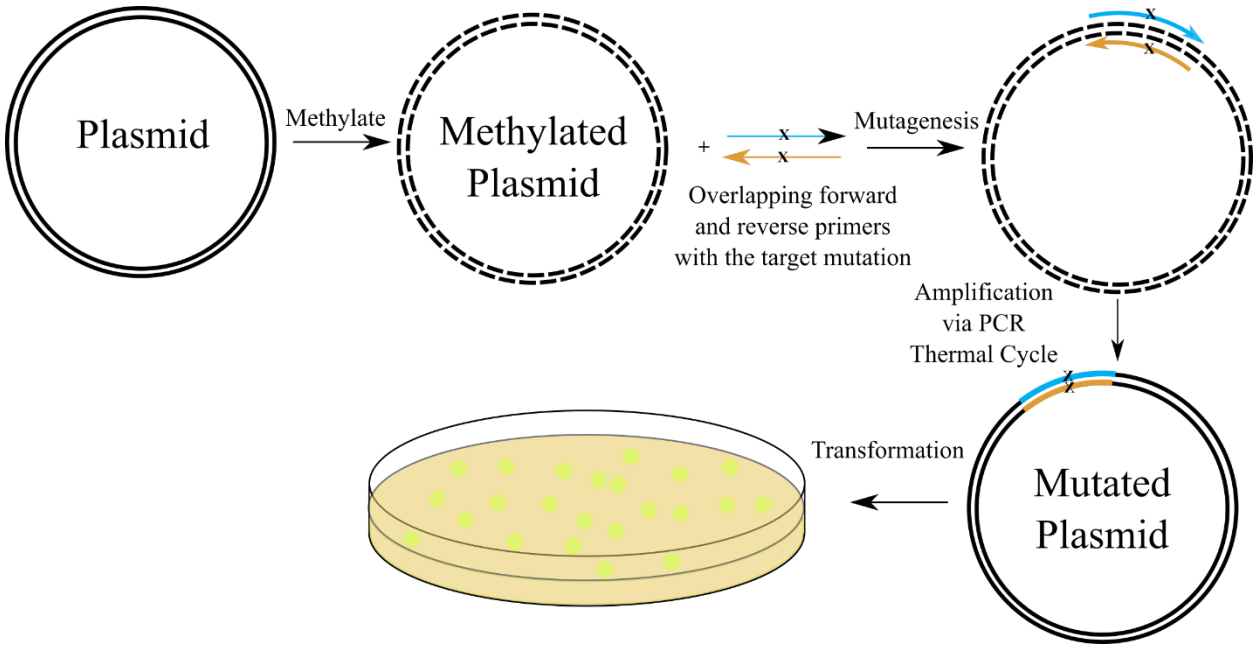

Figure 7: Site-Directed Mutagenesis Work-Flow. Parental plasmid (pGEX-6P-2 with rat FABP1 cDNA) is methylated and undergoes a mutagenesis reaction with mutagenic primers within the thermal cycler. The resulted mutated plasmid is transformed into competent cells using by heat shocking. Bacterial cells are selected for by streaking on agar containing 100 µg/mL ampicillin.

Figure 8: Complementary Mutagenic Forward and Reverse Primers. Top sequence is the forward primer while the bottom is the reverse primer. DNA bases in yellow are the single nucleotide substitution resulting in the coding of alanine instead of the normal threonine.

Table 5: Reaction mixture for methylation and mutagenesis reaction

Reagent	Volume (µL)	Final Concentration
10x AccuPrime Pfx Reaction Mix	5	1X
10X Enhancer	5	1X
Forward Primer (10 µM)	1.5	0.3 µM
Reverse Primer (10 µM)	1.5	0.3 µM
Plasmid DNA (20 ng/µL)	1	20 ng
DNA Methylase (4 U/µL)	1	4 units
25X SAM	2	1X
AccuPrime Pfx (2.5 U/µL)	0.4	1 unit
PCR water	32.6	-

Table 6: Thermal cycling settings for the methylation and mutagenesis of pGEX-6P-2 with rat FABP1 cDNA

Temperature (°C)	Duration (Minutes)	Number of Cycles	Stage
37	20	1	1
94	2		
94	0.33	18	2
65	0.5		
68	2.5		
68	5	1	3
4	∞		

Table 7: Recombination reaction mixture

Reagent	Volume (µL)	Final Concentration
PCR Water	10	-
PCR Sample	4	-
5X Reaction Enzyme Buffer	4	1X
10X Enzyme Mix	2	1X

ice. For the transformation step, DH5α-T1^{R} competent cells were used to take up the mutagenic plasmid.

Vials of 50 µL DH5α-T1^{R} were thawed on wet ice for 7 minutes with the direct addition of 2 µL of the recombination reaction to the competent cell vials. Contents of the vial was gently mixed by tapping and incubated on ice for 12 minutes. Vials were then quickly transferred into a 42°C water bath for 30 seconds. Vials were removed from the water bath and placed onto wet ice for 2 minutes and then 250 µL of pre-warmed SOC media was added to each vial. Samples were further diluted when 8.3 µL of the recombination reaction was added to 91.7 µL of SOC media. Diluted samples were added to agar plates with 100 µg/mL ampicillin and cells were spread on agar with plating beads by vigorously shaking the plate in a circular clockwise and counter clockwise motion for 1 minute each. Plates were inverted and incubated at 37°C overnight (16 hours). To validate the mutants, the DNA plasmid was sent to the Manitoba Institute of Cell Biology for DNA sequencing using pGEX 3' Sequencing Primer, 5'.

Recombinant FABP1 and T94A Expression

Rat FABP1 cDNA contained within the plasmid vector pGEX-6P-2 was changed into having the missense mutation Adenine (A) → Guanine (G) resulting into a Threonine (Thr) → Alanine (Ala) at position 94. This mutated plasmid vector was transformed into *E.* coli DH5α cells for large scale production of the FABP1 T94A variant. Glycerol stocks of FABP1 T94A were streaked on agar containing 100 µg/mL ampicillin and incubated overnight (16 hours) at 37°C. Single colonies from the plate were inoculated in two 3 mL LB broth in 15 mL tubes with 100 µg/mL ampicillin and 20 mM dextrose as a starting culture. The starting culture was grown overnight by shaking (200 rpm) at 37°C. After the growth of the starting culture, 5 mL was

diluted into 500 mL LB broth (with the previous mentioned supplements) contained in 2.8 L Erlenmeyer flasks.

The large batch culture was grown for 5-6 hours at 37°C with 200 rpm to reach an OD_{600} ≈ 1.0. To induce the expression of FABP1 T94A, 1 mM of isopropyl-β-D-thio-galactoside (IPTG) (Invitrogen, ThermoFisher Scientific, Mississauga, Canada) was added to the large batch culture. The large batch culture was grown for an additional six hours incubating at the same conditions to induce the expression of the protein. Cells were collected by centrifugation at 3500 g for 20 minutes removing the supernatant and resuspending cells with 20 mL of cold 1 X PBS containing 1% Triton X-100 and protease inhibitors (phenylmethylsulfonyl fluoride (PMSF), aprotinin, and leupeptin at concentrations of 25 µg/ml, 2 µg/ml, 1 µg/ml respectively). 20 mL of cell suspension was sonicated using the Sonifier 450 (Branson, fisherscientific, ThermoFisher Scientific, Mississauga, Canada) with ½ inch disrupter horn set at hold, a duty cycle of 50%, and an output dialed at 3.5. Cells were kept on ice and sonicated for 30 seconds and rested for 30 seconds for a total of five times. Cellular debris were centrifuged down at 12,000 g for 20 minutes at 4°C and the soluble protein fraction was collected.

Recombinant FABP1 and T94A Purification

FABP1 and the T94A variant were purified from the cell lysate using the ÄKTA Fast protein liquid chromatography (FPLC) and GSTrap Fastflow (FF) columns (GE Life Sciences, Chicago, USA). The workflow of the purification of FABP1 and T94A is shown in Figure 9. Air bubbles in the ÄKTA FPLC were removed manually with a syringe. The system was pumped with water to wash before purification. The GSTrap FF columns were equilibrated with 5 column volumes (25 mL) of Binding buffer (1X PBS, pH 7.3) at 5 mL/min. Sample was loaded

into the column at 1 mL/min and the column washed with 10 column volumes (50 mL) of binding buffer at 5 mL/min. Proteins were eluted with elution buffer (50 mM Tris-HCl, 10 mM reduced glutathione, 1 mM DTT, pH 8.0).

The eluted protein sample was cleaved with the addition of 500 µL PreScission Protease (GE Life Sciences, Chicago, USA; 40 µL PreScission Protease and 460 µl of cleavage buffer [50 mM Tris-HCl, 150 mM NaCl, 1 mM EDTA, 1 mM dithiothreitol (DTT), pH 7.5]). The eluted fusion protein was incubated with protease at 4°C overnight with end over end rotation. After digestion, protein samples were re-added to an equilibrated GSTrap FF column with a syringe. The flowthrough containing FABP1 or T94A variant was collected while the GST tag and PreScission protease stayed in the column. Protein samples were then concentrated using Amicon Ultra- 15 Centrifugal Filter Devices. Eluted proteins (12 mL) were added into the device and centrifuged at 5,000 g for 60 minutes.

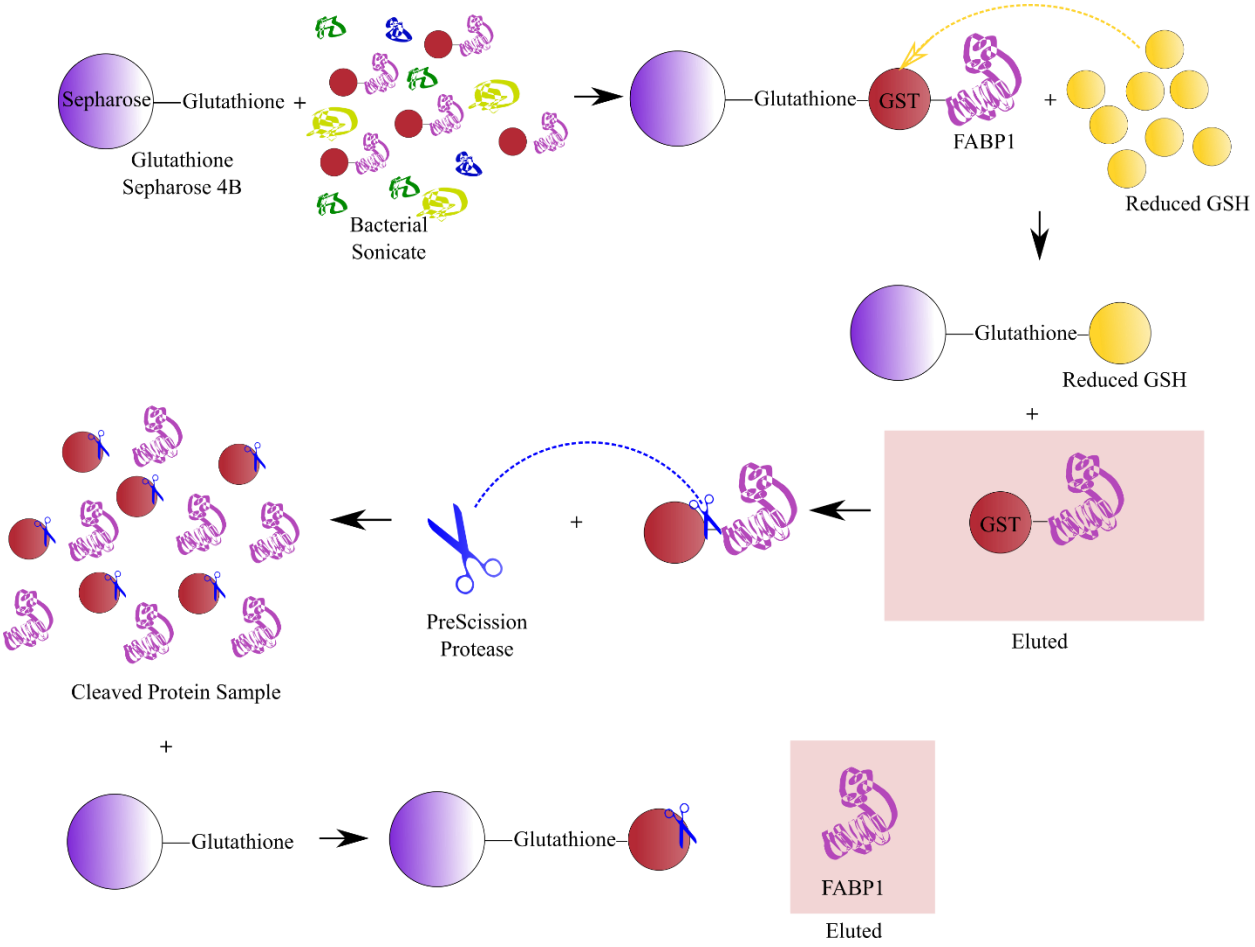

Figure 9: Workflow of the purification of recombinant rat FABP1 and the T94A variant. Bacterial sonicate is added in a GSTrap FF where only the fusion protein (GST with FABP1/T94A) can bind to the column due to the affinity for glutathione attached to Sepharose in the column. All other contaminants are washed out of the column. The fusion protein is eluted where it is cleaved by PreScission Protease. The protein sample is re-added onto the column to remove the GST tag leaving FABP1 and its variant in the flow through.

Bradford Assay

The Bradford Assay was used as a colorimetric method to rapidly and accurately estimate total protein concentration. This assay is simple, fast and more sensitive than the Lowry assay. The Bradford assay uses Coomassie Brilliant Blue G-250 (Bio-Rad, Hercules, USA) dye that has three forms: the acidic red cation, neutral green, and blue anion. These forms can be detected at absorbance maxima at 470, 650, and 595 nm, respectively. The blue form occurs when the dye binds with the protein allowing for the estimation of protein quantity.

The Coomassie Reagent solution (ThermoFisher Scientific, Mississauga, Canada) was mixed by inverting the bottle before use and 5 µL of the protein sample or standard was pipetted into a microwell plate (Sarstedt, Saint-Léonard, Canada). Coomassie reagent was added to each well (250 µL) and the microplate was mixed on a shaker for 30 seconds. The plate was then incubated for 10 minutes at RT. Absorbance was read at 595 nm after the incubation period in a microplate reader (Synergy HT, Vermont, BioTeK).

Sodium Dodecyl Sulfate Polyacrylamide Gel Electrophoresis (SDS-PAGE)

SDS-PAGE was used to confirm the identity of the purified recombinant protein. A 15% separating and 5% stacking gel were used for the SDS-PAGE and Western blot. The composition of the separating and stacking gel are listed in Table 8. A long glass plate with 1.5 mm spacers was put together with a short glass plate in a casting frame. Plates were made such that they were flush before closing the casting frame. The casting frame with the plates was inserted into

Table 8: Components mixed for making a 15% separating gel and a 5% stacking gel

Reagent	Separating Gel (15%)	Stacking Gel (5%)
Double Distilled Water	2.3 mL	3.4 mL
Tris-HCl (1.5M and 1M respectively)	2.5 mL	0.63 mL
SDS (10%)	100 µL	50 µL
Acrylamide Mix (30%)	2.5 mL	0.83 mL
Ammonium Persulfate (APS) (10%)	100 µL	50 µL
TEMED	4 µL	5 µL

the casting stand that has a strip of Parafilm on top of a foam piece to prevent leakage when adding solutions. Leakage was checked by adding small amounts of water between the glass plates. The water was discarded by inverting the whole apparatus and dried using square pieces of filter paper. The separating gel solution was added using a transfer pipette and a layer of isopropanol was added on top of the separating gel solution to act as a seal. The separating gel was allowed to solidify for 30 minutes before the sealant was poured off. The stacking gel solution was carefully layered on top of the hardened separating gel making sure to not introduce any air bubbles before inserting in the sample comb. The stacking gel was allowed to set for 15 minutes.

The gel cassette was removed from the casting frame and inserted into an electrode assembly with either another gel cassette on the other side or a dummy plate. Running buffer (25 mM Tris, 190 mM glycine, 0.1% SDS) was poured into the electrode assembly (250 mL) and the sample comb was carefully removed. Electrode assembly was placed in the electrophoresis tank that was filled 1/3 with running buffer. A total of 30 µg of protein (15 µL) was added to (5 µL) 4x sample loading buffer (250 mM Tris-HCl pH6.8, 20% glycerol 8%, sodium dodecyl sulfate (SDS), 0.2% bromophenol blue, and 5% β-mercaptoethanol). Samples were boiled for 5 minutes at 100°C and briefly spun down with a Mini Centrifuge ((Mandel Scientific, Ontario, Canada). Samples were loaded into the wells (20 µL) and the tank's lid was closed. Electrophoresis was performed at a constant 100 Volts for 90 minutes using the Miniprotean II cell powered by Powerpac 1000 (Bio-Rad, Hercules, USA). At the end of the run, the stacking gel was removed using the gel releaser or a scalpel. The gel was washed with water a total of three times before being submerged in Coomassie stain (0.1% Coomassie R-250, 10% acetic acid, 40% methanol). The gel in the Coomassie stain solution was heated in the microwave oven for 1 minute and

gently agitated (Thermolyne Slow Speed Roto Mix) for 15 minutes. To destain the gel, the stain solution was replaced with distilled water, the gel was heated again in the microwave oven for 2 minutes, and rocked for 30 minutes with balls of Precision Wipes (Kimberly-Clark Professional, Roswell, USA). The Precision Wipes were removed and the step was repeated 3-4 times until the gel was destained enough to view the bands.

Western blot

Western blot was another method used to confirm identity of the purified recombinant protein. Gel, sample preparation, and electrophoresis followed the same steps in SDS-PAGE but instead of staining the gel with Coomassie stain solution the gel is floated into 1X transfer buffer (25 mM Tris, 190 mM glycine, 20% methanol) before being assembled into a transfer cassette for 30 minutes at 4°C. The transfer cassette components, foam pads and filter papers were incubated in transfer buffer 1 hour before assembling and initiating the electroblotting. The 0.45 µm nitrocellulose membrane (Bio-Rad, Hercules, USA) was submerged in 1X transfer buffer for 10 minutes. The transfer cassette was assembled as followed: black sided cassette, foam pad, filter paper, gel, membrane, filter paper, sponge, and clear sided cassette. Extra care was taken when handling the components of the sandwich such as handling the gel with a spatula and blunt tweezers with the membrane. The bubbles were rolled out with a glass rod before closing the sandwich cassette.

The sandwich was placed in the electrode with the black side together. The assembled electrode housing the cassette was inserted in the chamber filled to the 2 gel mark with transfer buffer and a magnet spinner. The chamber was closed and placed in a plastic container that was then filled with ice. The plastic container was placed on top of a magnet stirrer and the blot was

run for 1 hour at 100 Volts. After, the sandwich was disassembled and the membrane was rinsed in water three times before being blocked with 5% (w/v) non-fat skim milk in Tris buffered saline with Tween 20 (TBST) solution (20 mM Tris pH 7.5, 150 mM NaCl, 0.1% Tween 20) for 1 hour at RT with gentle agitation. The blocking solution was prepared a day earlier to fully dissolve the skim milk. After blocking, the liquid was decanted and the membrane was washed three times with 30 mL 1X TBST for 5 minutes. The membrane was then incubated with 10 mL rabbit polyclonal L-FABP antibody (Santa Cruz Biotechnology, Dallas, USA) (1:500 in 5% powdered non-fat skimmed milk in TBST) overnight with gentle agitation. After the application of the primary antibody, the membrane was washed five times with 30 mL of 1X TBST for 5 minutes each. The membrane was then incubated with goat anti-rabbit IgG-horseradish peroxidase (Santa Cruz Biotechnology, Dallas, USA) (1:500 in TBST) for 1 hour at RT with gentle agitation. After incubation with the secondary antibody, the membrane was washed five times with 30 mL TBST for 5 minutes each. Samples in the membrane were detected by enhanced chemiluminescence using the ECL Plus system from GE Lifesciences. Contents of the kit were incubated at RT for 20 minutes. Reagents A and B were then mixed in a one to one ratio (5 to 5 mL). The mixture was added to the membrane in a plastic container shielded by aluminum foil and incubated for 5 minutes at RT. The membrane was then held by blunt forceps and dabbed on the corner to Precision wipes to remove excess solution. The membrane was visualized in an Alpha Innotech FluorChem FC2 MultiImage If with a development time of 10 minutes, speed/resolution at medium/high, and chemical blot selected. Protein samples were also sent to the Pharmaceutical Analysis Laboratory at the University of Manitoba for liquid chromatography mass spectrometry to confirm protein size.

Dichlorofluorescein (DCF) Fluorescence Assay

A DCF assay was used in determining whether FABP1 T94A variant possesses the antioxidant capacity similar to that of the non-mutant protein. The DCF assay uses a fluorescence probe to indirectly measure the amount of ROS *in vitro*. The compound 2, 7-dichlorofluorescein-diacetate (DCFH-DA) was de-esterified by reacting with ethanol and sodium hydroxide yielding 2, 7-dichlorodihydrofluorescein (DCFH). This non-fluorescent derivative is the dye stock solution prepared fresh by mixing 0.5 mL of 0.01 N NaOH with 125 µL 1.5 mM DCFH-DA in ethanol at RT in the dark for 30 minutes. The addition of 2.5 mL of 20 mM sodium phosphate buffer (pH 7.0) neutralizes the dye stock. The DCFH is a compound when oxidized by ROS produces the fluorescent compound dichlorofluorescein (DCF). DCF can be measured at an excitation of 485 and emission at 590 nm. Figure 10 shows the chemical reaction the parent compound DCFH-DA undergoes to produce DCF. The introduction of antioxidants in the reaction would prevent DCF from forming due to the antioxidants reacting with ROS. Oxidation reactions were performed in 96 well CoStar plates where 50 µL of different concentrations protein sample or control is added to 40 µL DCFH [60 µM], 5 µL iron (II) sulfate ($FeSO_4$) [1 mM], and 5 µL hydrogen peroxide (H_2O_2) [1 mM]. Sample fluorescence were read in a microplate reader (Synergy HT, BioTeK) at an excitation of 485 and emission at 590 nm.

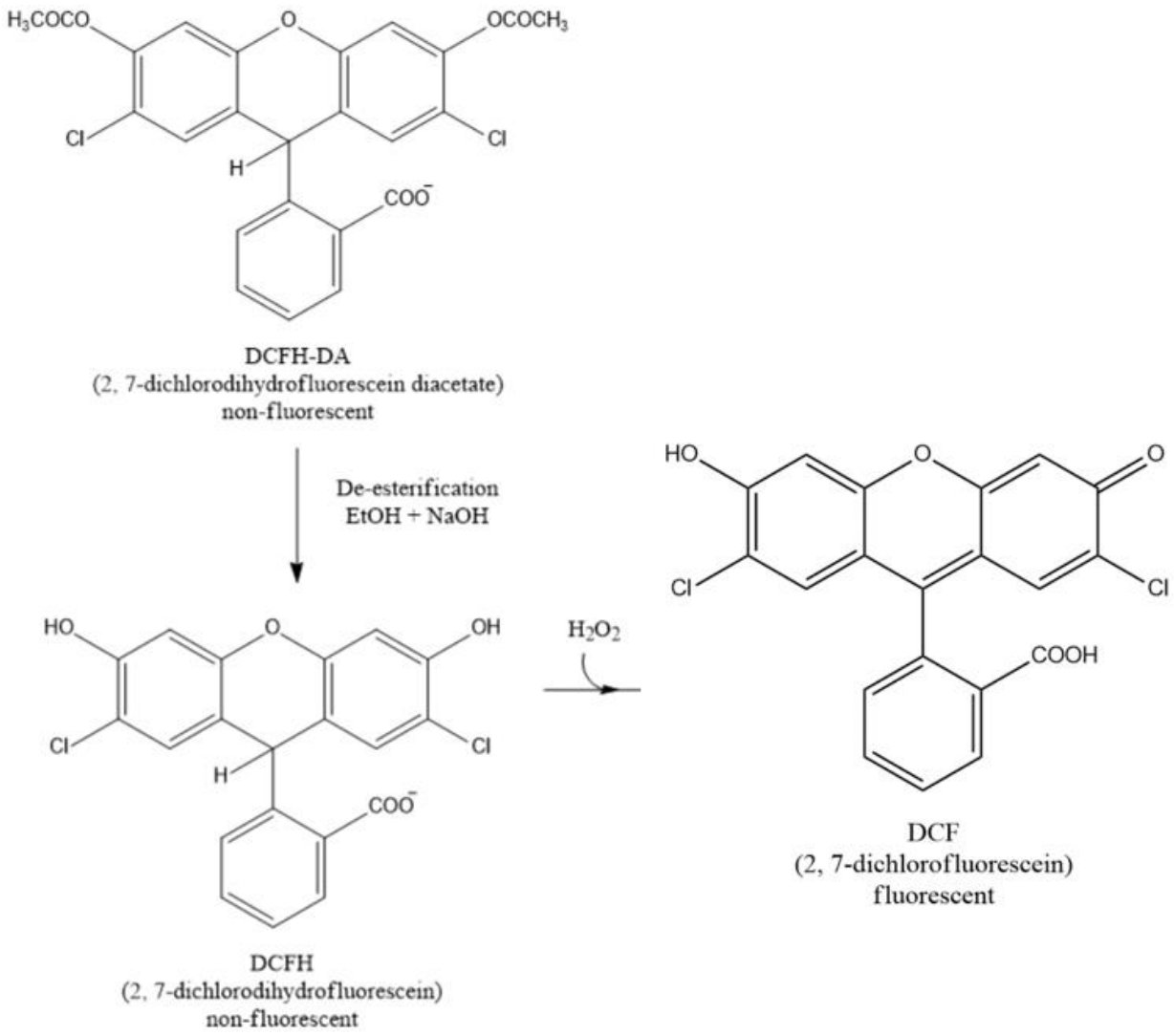

Figure 10: Chemical reaction of the DCF assay. DCFH-DA is de-esterified by ethanol and sodium hydroxide into DCFH. DCFH is a compound that can be oxidized by ROS to produce the highly fluorescent DCF that can be measured.

Thiobarbituric Acid Reactive Substances (TBARS) Assay

Indications that oxidative stress is occurring in cells are the presence of lipid peroxides that decompose into reactive compounds such as MDA. The secondary products of lipid peroxidation are considered markers of oxidative stress thus, these compounds when measured can illustrate the capacity of a protein to act as an antioxidant. The TBARS assay is a method to measure lipid peroxidation by determining MDA levels. Figure 11 shows the chemical reaction between MDA and thiobarbituric acid (TBA) forming a 1:2 adduct that can be colorimetrically measured. To generate lipid peroxides, low density lipoproteins (LDL) are incubated with azo compounds. Figure 12 shows the azo compounds 2, 2'-Azobis (2-methylpropionamidine) dihydrochloride (AAPH) and 2,2'-Azobis(4-methoxy-2,4-dimethylvaleronitrile) (MeO-AMVN) that release free radicals in a hydrophilic and hydrophobic environment, respectively. These azo compounds thermally decompose into free radicals. The free radicals would then attack the LDL releasing lipid peroxides where MDA would be derived. For the TBARS assay, malondialdehyde bis (dimethyl acetal 1, 1, 3, 3-tetramethoxypropane) was prepared fresh and used as a standard. LDL [0.5 mg/mL] was incubated with either AAPH [10 mM] or MeO-AMVN [1 mM] and with varying concentrations of protein in a 37°C water bath for 90 minutes. The addition of TBA solution (0.67% TBA, 15% trichloroacetic acid, 0.25 N HCl) halts the oxidation reaction and samples were then heated at 100°C for 15 minutes to develop the colorimetric pink chromogen. The reactions were then cooled on ice for 5 minutes and centrifuged briefly to pellet the flocculates. Samples were then pipetted into a 96-well microplate and the absorbance was read at 535 nm using a spectrophotometer.

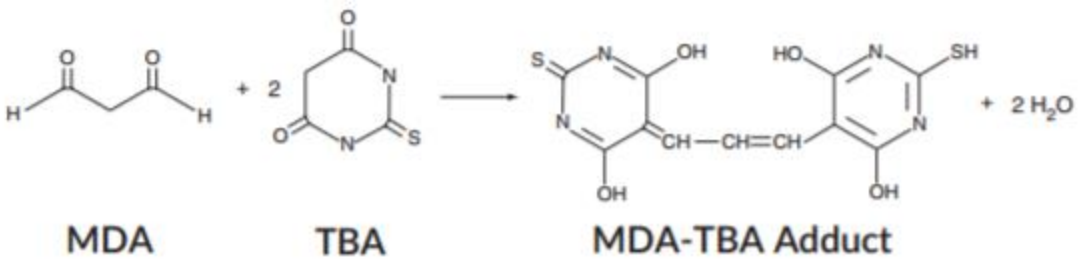

Figure 11: The chemical reaction of between MDA and TBA to form the 1:2 MDA-TBA Adduct.

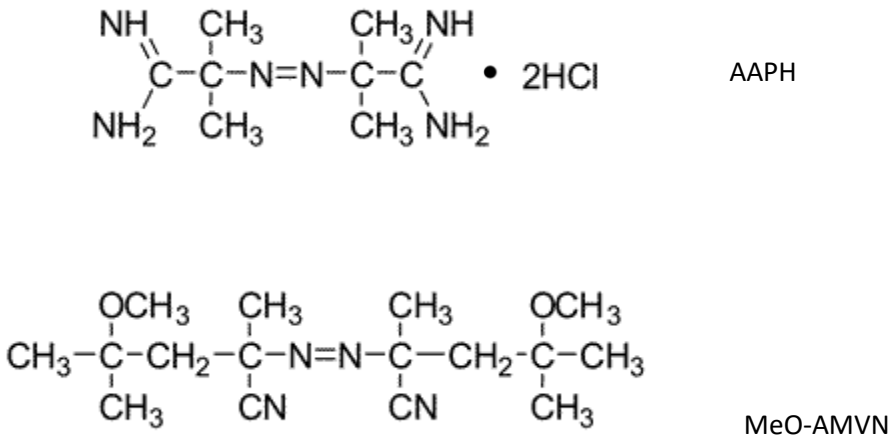

Figure 12: Chemical structures of the used azo compounds. The top chemical structure is the water-soluble azo compound, AAPH which was used to release free radicals in a hydrophilic environment. The bottom structure shows MeO-AMVN, which releases free radicals in a lipophilic environment.

The TBARS assay was also used to evaluate whether the proteins were affected by binding with fatty acids palmitate and alpha-bromo palmitate. For this experiment 10 µM of the proteins were pre-incubated with the fatty acids at a concentration of 30 µM for 1 hour before being subjected to the oxidation reactions.

Statistical Analysis

Data are presented as mean ± SEM. The N value is the number of replicates for each study. Statistical analyses used t-test (unpaired) where two groups were compared while a two-way ANOVA was used for multiple comparisons followed by a Bonferroni post-test using GraphPad Prism 6.0. Results were considered significant when the p-value was less than 0.05.

Chapter 3: Results

Identification of the Plasmid Vector pGEX-6P-2 Encompass FABP1 cDNA by Restriction Enzyme Mapping

Restriction enzyme mapping was performed for determining whether bacterial stocks contained the correct plasmid vector with the FABP1 cDNA (Figure 13). FABP1 cDNA was initially ligated into the pGEX-6P-2 vector with BamHI and XhoI restriction enzyme recognition sequences (Yan *et al*., 2009). By using these endonucleases the isolated plasmid can be cleaved into the vector and the cDNA. Agarose gel electrophoresis permits the separation of the DNA into bands of appropriate sizes. As illustrated in Figure 13, there is a separation between the plasmid vector at an estimated 4900 bp and the FABP1 cDNA at 418 bp. Knowing that the bacterial stocks comprise the required FABP1 cDNA inserted at the correct location in the plasmid vector, the plasmid can be used to introduce the point mutation by site directed mutagenesis. Figure 14 shows the comparison between the original and the mutated plasmid. There is no difference between the original and mutated pGEX-6P-2 and FABP1/T94A bands, suggesting no unnecessary deletions or insertions occurred during the site directed mutagenesis.

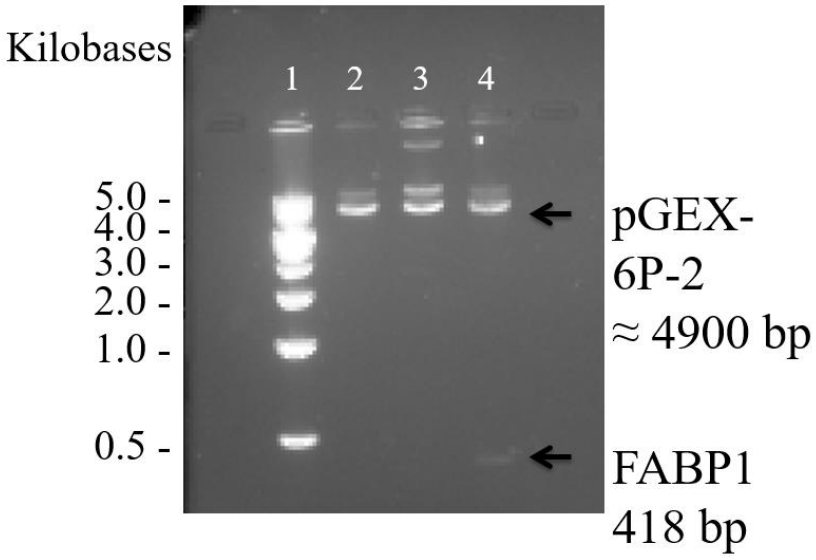

Figure 13: Analysis of recombinant pGEX-6P-2/FABP1 using restriction enzyme digestion. Plasmids were purified using the plasmid midi kit from QIAGEN and digested with endonucleases at 37°C for 4 hours. DNA samples were loaded onto 1.0% agarose gel which ran for 90 minutes at 100 V. The gel was stained with SYBR Safe and visualized with a UV transilluminator. The gel shows DNA ladder (1) with the original pGEX-6P-2 FABP1 plasmid digested with BamH1 (2), Xho1 (3), and BamH1 and Xho1 (4).

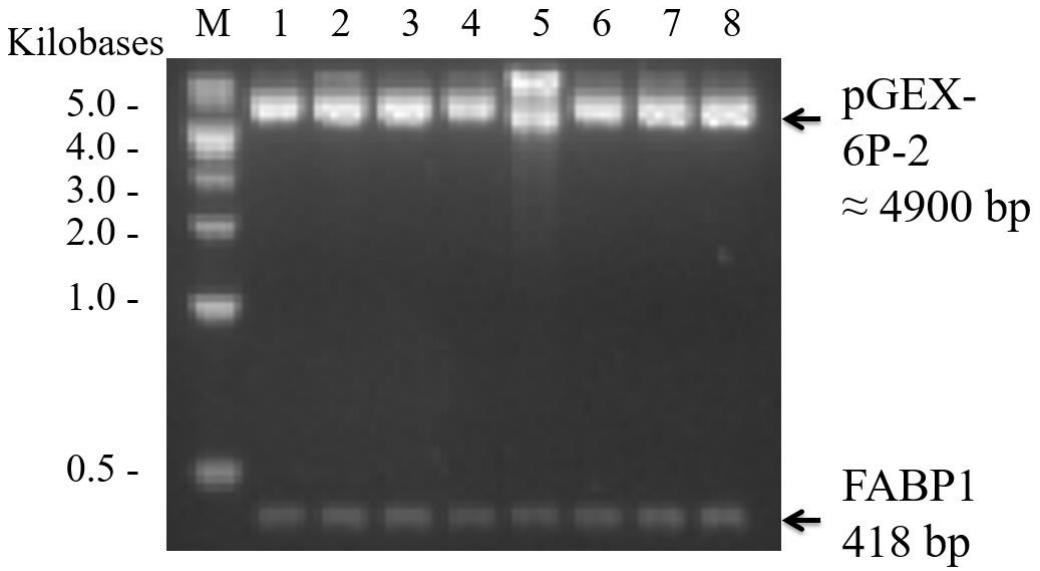

Figure 14: Analysis of recombinant pGEX-6P-2/FABP1 using restriction enzyme mapping after site-directed mutagenesis using GENEART Site Directed Mutagenesis System. Plasmids were purified using the plasmid midi kit from QIAGEN and digested with endonucleases at 37°C for 4 hours. DNA samples were loaded into 1.0% agarose gel which ran for 90 minutes at 100 V. The gel was stained with SYBR Safe and visualized with a UV transilluminator. Lanes 1 and 2 show the original plasmid while the mutated plasmid that were digested with BamH1 and Xho1 are in lanes 3-8 pGEX-6P-2/FABP1.

The Confirmation of the Plasmid Vector pGEX-6P-2 with FABP1 cDNA by DNA Sequencing

While the restriction enzyme mapping of the mutated plasmid showed no changes in the size of the DNA after introducing a point mutation, further confirmation was needed at the DNA level. DNA sequencing was performed on isolated, non- and mutated plasmids to show that the correct mutation was induced. Figure 15 shows the comparison of two sequences, the non-mutated rat cDNA sequence at the top (Query 1) and the mutated (Subject). Indicated by the red box is the mutation where a nucleotide adenine is changed into a guanine coding from a threonine to an alanine protein residue at the 94^{th} position. With the required mutation confirmed, purification of the protein can commence.

Expressing Recombinant proteins FABP1 and the FABP1 T94A Mutant Variant

The plasmids used in this study contained FABP1 and the mutated variant T94A cDNA fragments. The fragments are located between restriction enzymes site BamHI and XhoI, which is downstream of a GST tag sequence. The promoter for the GST tag can be induced by introducing IPTG to the bacterial culture. When bacteria was being cultured, 1 mM of IPTG was added to the flasks and incubated for another 6 hours before collecting the cells. Figure 16A shows a 15% SDS-PAGE gel comparing non- and mutated bacterial sonicates without or with bacterial induction with IPTG. From the figure, the dark band indicated by the arrow at 40 kDa is the fusion protein: FABP1 or T94A with the GST tag. Lanes 2 and 4 show that the band is darker than lanes 1 and 3 due to having IPTG. Figure 16B illustrates a histogram of the band density the gel seen in Figure 16A using ImageJ for analysis.

Figure 15: The DNA sequence of the non-mutated plasmid compared to mutated sequence. The top strand (Query 1) is the non-mutated rat FABP1 cDNA sequence from http://uswest.ensembl.org/ plasmid while the bottom strand (Subject) is the mutated. Highlighted by the red box is the point mutation where the adenine is replaced by guanine. This results in the variant where the protein residue threonine is substituted for an alanine. The sequence of the mutated plasmid was sent to the Manitoba Institute of Cell Biology for sequencing with pGEX 3' Sequencing Primer, 5'.

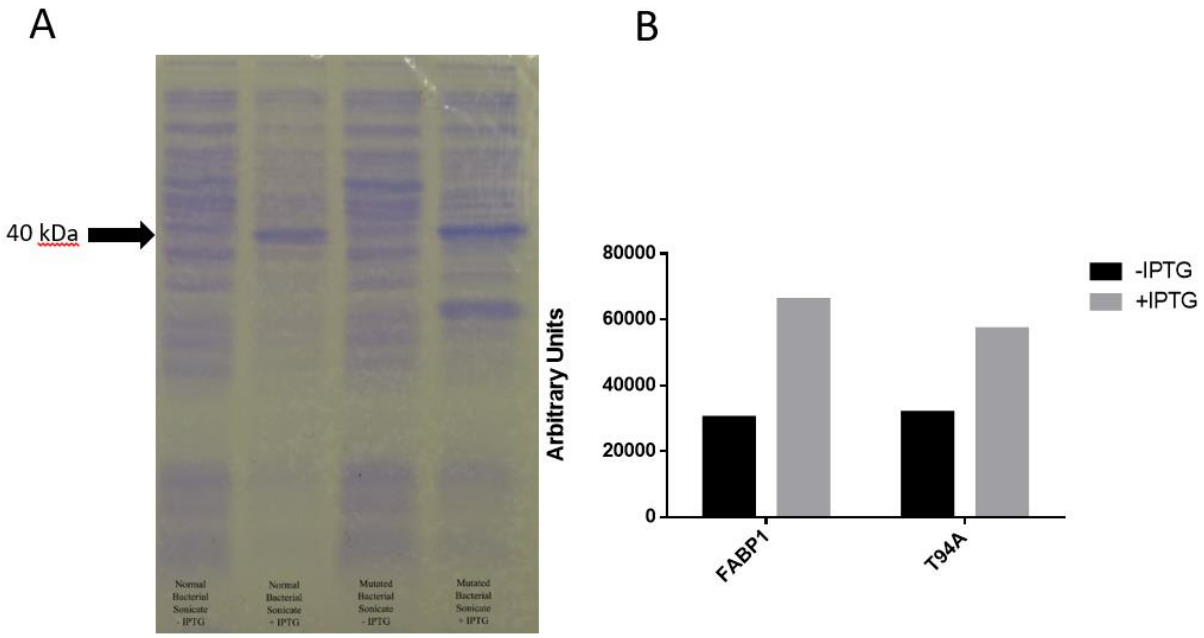

Figure 16: Protein induction with IPTG. (A) A 15% Tri-Glycine SDS-PAGE gel. From left to right: Normal bacterial sonicate, induced normal bacterial sonicate, mutated bacterial sonicate, induced bacterial sonicate. (B) Histogram illustrating the band density of a 15% Tri-Glycine SDS-PAGE gel of Figure 16A between induced and uninduced bacterial cultures.

From Figure 16B, samples that were induced with IPTG have clearly stronger band densities compared to samples that were uninduced with IPTG.

The Purification of Recombinant FABP1 and FABP1 T94A

The fusion protein was purified and the GST tag was separated from FABP1 or the T94A variant with PreScission protease. Figure 17 shows a 15% polyacrylamide gel loaded with AmerchamTM ECLTM RainbowTM Marker- Full Range, normal bacterial sonicate, induced normal bacterial sonicate, mutated bacterial sonicate, induced bacterial sonicate, normal fusion protein, mutated fusion protein, FABP1, and the T94A variant protein. In Figure 17A, lanes 6 and 7 show both the non-mutated and mutated fusion proteins having a size of 40 kDa. The size of the fusion protein comes from the GST tag having a size of 26 kDa and the FABP1 and T94A having a size of 14 kDa. The next two lanes show purified recombinant proteins at 14 kDa after cleavage and additional purification to remove the tag and the protease. It can be seen that in the last four lanes there are no contaminants despite loading up to 30 µg of protein in each well. To further confirm the identities of the purified proteins a western blot was conducted.

Figure 17 B shows the western blot of the purified recombinant proteins. The result shows that the recombinant protein samples are immunoreactive with the rabbit polyclonal antibody against rat FABP1. Another method used to identify the purified proteins is to use LC-MS to determine the proteins' mass. Figure 18 is the total ion count chromatogram and the deconvoluted mass of FABP1 (A) and T94A (B). The deconvoluted mass of FABP1 was 1468 da and the T94A was 1438 da showing a difference of 30 da.

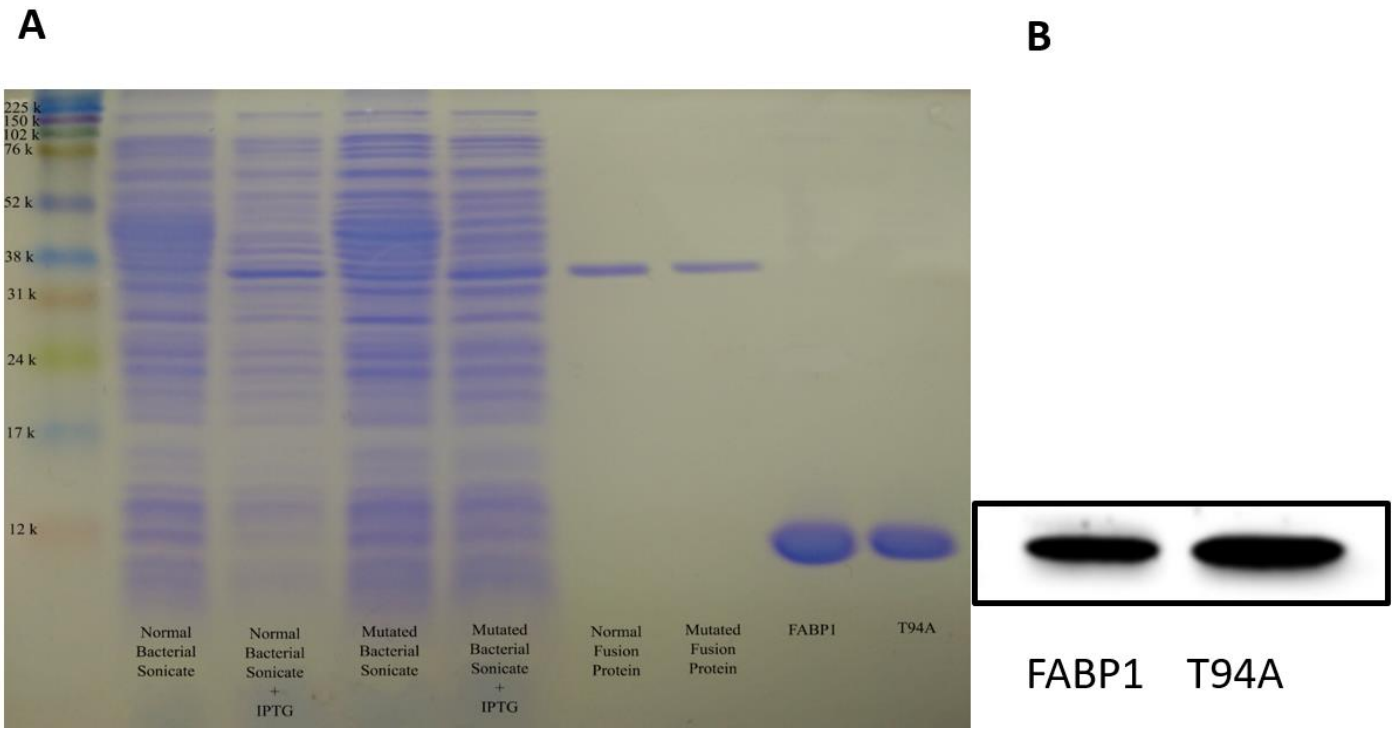

Figure 17: Identification of Proteins using SDS-PAGE and Western Blot A) 15% Tri-Glycine SDS-PAGE gel. From left to right: AmerchamTM ECLTM RainbowTM Marker- Full Range, normal bacterial sonicate, induced normal bacterial sonicate, mutated bacterial sonicate, induced mutated bacterial sonicate, normal fusion protein, mutated fusion protein, FABP1, and the T94A variant protein. B) Western Blot of the FABP1 and T94A variant proteins.

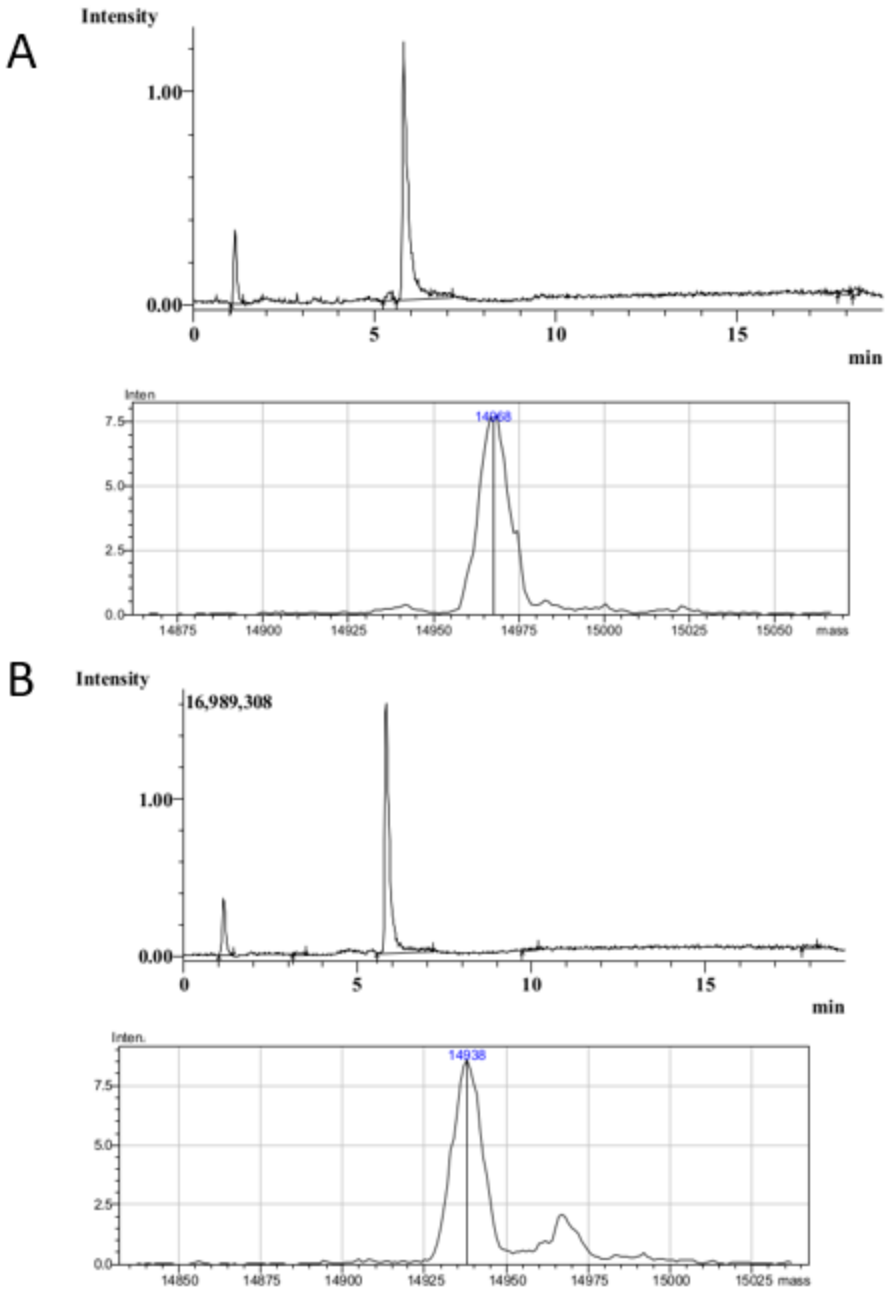

Figure 18: LC-MS Results. Total ion count chromatograms (top) and the deconvoluted mass (bottom) of FABP1 (A) and FABP1 T94A (B). Samples were sent to the Pharmaceutical Analysis Laboratory at the College of Pharmacy of the University of Manitoba for LC-MS.

Protein Quantification

A Bradford assay was used to quantify the purified recombinant proteins. Quantifying the proteins allows for further downstream studies. The Bradford assay uses Coomassie Brilliant Blue G-250, which shifts absorbance when binding to proteins. A blue colour results from the binding of the Coomassie reagent to the protein that can be measured at an absorbance of 595 nm. Sample absorbance readings can be used to calculate protein concentration using a standard curve. Bovine serum albumin was used as a standard where known concentrations of protein gave a resulting absorbance. By plotting the absorbance values and protein concentration of bovine serum albumin a standard curve is generated. The standard curve produced from using bovine serum albumin is shown in Figure 19 with the formula used for calculating the concentration of the purified recombinant proteins. Determining the values of the purified proteins was critical in the next few studies.

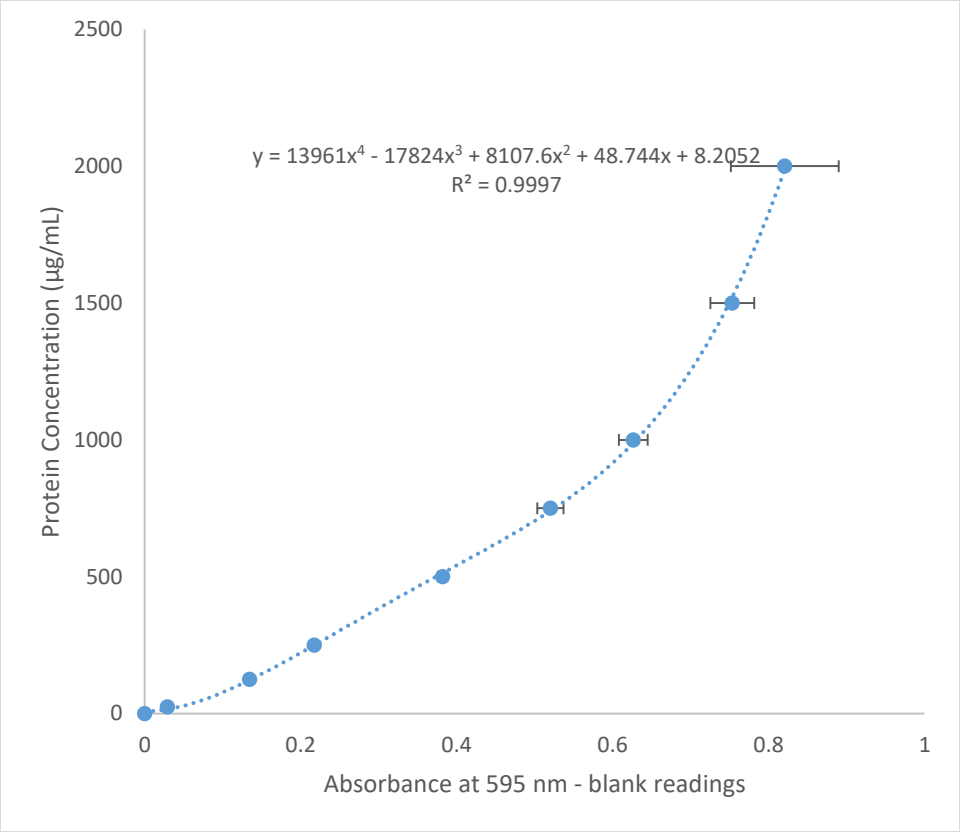

Figure 19: BSA standard curve to measure the total cell protein concentration. Data are presented as mean ± SEM (n = 3).

Screening the Antioxidant Capacity of Recombinant FABP1 T94A Using the DCF Fluorescence Assay

One of the main objectives of this study was determining whether recombinant rat FABP1 T94A variant possesses the ability to act as an antioxidant similar to its non-mutated form. To evaluate the protein's capacity to act as an antioxidant, the DCF fluorescence assay was employed. The assay used H_2O_2 and Fe_2SO_4 as a source of ROS while DCFH was used to measure levels of ROS as it reacts with these unstable molecules to produce the fluorescent DCF. Introducing antioxidants to this *in vitro* reaction will decrease the DCF fluorescence as they would reduce the amount of ROS in the system as seen with controls FABP1, ascorbic acid, and TROLOX™. Figure 20 shows results of the assay. At the lowest concentration of T94A (1 µM), the protein was able to reduce DCF fluorescence to 75.8 ± 2.9 while at its highest tested concentration of 20 µM a reduction to 36.3 ± 2.2% of the control was seen ($P< 0.001$). Increasing the concentration of antioxidants was associated with a decrease in DCF fluorescence. When comparing T94A to FABP1, there were no significant differences in their ability to reduce DCF fluorescence at all concentrations.

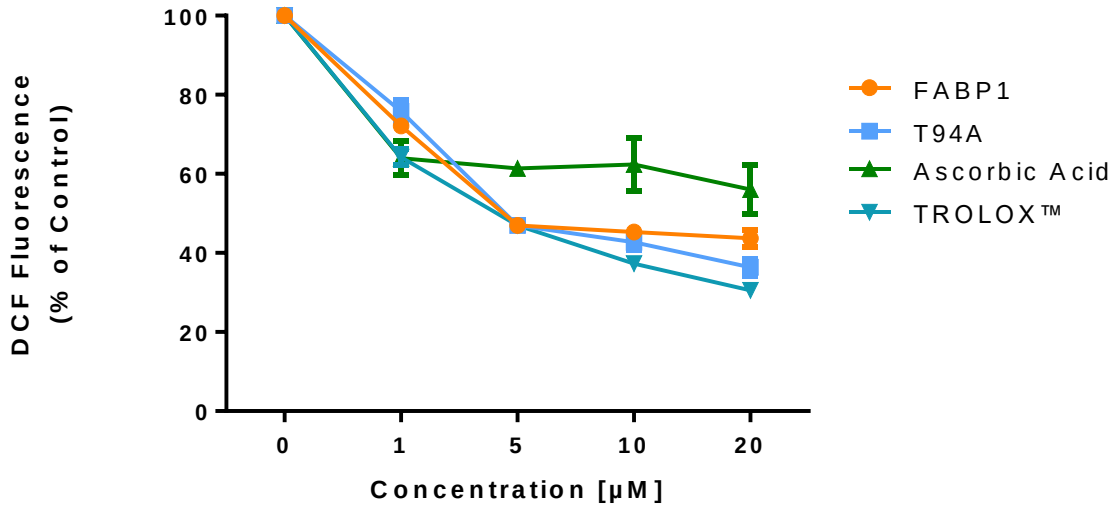

Figure 20: DCF fluorescence intensity versus antioxidants recombinant FABP1, FABP1 T94A, ascorbic acid, and TROLOX™ concentration. The parent compound DCFH-DA was de-esterified to the dye stock DCFH that was used to detect ROS in the reactions. Reactions was conducted in 96 well CoStar plates with 24 µM DCFH, 50 µM FeSO4, 50 µM H2O2, and protein sample. Data are presented as mean ± SEM (n = 4). Statistical difference ($p<0.05$) was determined between control (0 µM antioxidant) and different levels of antioxidants.

The Effect of Recombinant FABP1 T94A on *in vitro* Lipid Peroxidation with AAPH and MeO-AMVN

To further evaluate the performance of the FABP1 T94A variant as an antioxidant, the protein could be able to display this function in hydrophilic and/or lipophilic environments. Free radical releasing systems were used to simulate these environmental conditions. AAPH and MeO-AMVN release free radicals when used with LDL. Since these compounds thermally decompose at different rates it was necessary to standardize their concentrations such that free radical release would be similar. Using a TBARS assay, LDL was incubated with 10 mM AAPH and was found to produce 670.09±13.4 ng MDA/ mg LDL protein (Figure 21). MeO-AMVN (1 mM) generated 713.0±11.2 ng MDA/ mg LDL protein and compared with AAPH was not significantly different between the amounts of MDA at these concentrations (Figure 21). Since these concentrations of azo compounds produced similar amounts of MDA they were used in determining T94A's performance as a hydrophilic and lipophilic antioxidant. Yan *et al*. (2009) found that FABP1 acts as both a hydrophilic and lipophilic antioxidant so the importance in determining whether the T94A mutation affects the protein's ability to act as an antioxidant in both cases is clear. Figure 21 established an appropriate *in vitro* system that gives the opportunity to observe the mutant's ability in hydrophilic and lipophilic conditions. The TBARS assay was done using 10 mM AAPH to generate water soluble ROS. Figure 22A shows that increasing T94A concentration inhibits MDA formation.

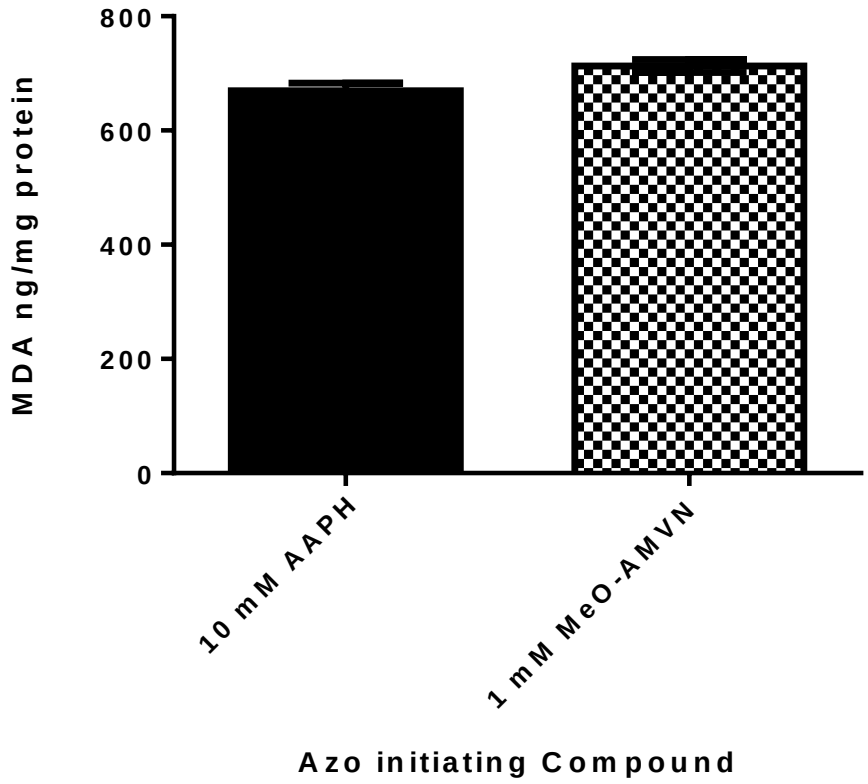

Figure 21: Equalizing the production of MDA for each azo compound. MDA formation of 10 mM AAPH and 1 mM MeO-AMVN with 0.5 mg/ml LDL. Azo compounds were incubated with LDL for 90 minutes in a 37°C water bath. MDA was assessed using the TBARS assay. Values are presented as means ± SEM, n = 4; P>0.05.

At a concentration of 20 µM, T94A produced 72.1±4.4% of the control MDA. In a lipophilic system that used 1 mM MeO-AMVN to produce ROS, the mutant protein was able to inhibit 23.4±5.5% of MDA from forming at 20 µM (Figure 22B). The T94A variant was able to reduce MDA in a dose-dependent manner in both environments (Figure 22A and 22B). Positive controls used for the assay included ascorbic acid and TROLOX™ in the AAPH system while in the MeO-AMVN system the ascorbic acid acted as a negative control. When comparing FABP1 to T94A when AAPH was used as a source of ROS, there was a significant difference between the two protein's at concentrations at 1 µM (79.8%±1.5 and 105.0%±9.4 of the control) and 10 µM (65.8%±1.8 and 88.1%±5.7 of control) ($P < 0.05$). However, the amount of MDA produced at 20 µM was similar (59.4%±6.8 and 76.6%±5.5 of control). When antioxidant activities of FABP1 and T94A were used in a lipophilic environment (1 mM MeO-AMVN) there was no statistical difference in MDA production (Figure 22B). Figure 23 shows a summary of the FABP and T94A data using AAPH and MeO-AMVN systems. The FABP1 T94A variant preformed similarly in both conditions. Figures 23 and 24 illustrate that FABP1 T94A is able to reduce MDA production in the AAPH induced hydrophilic free radical system and the lipophilic free radical system of MeO-AMVN.

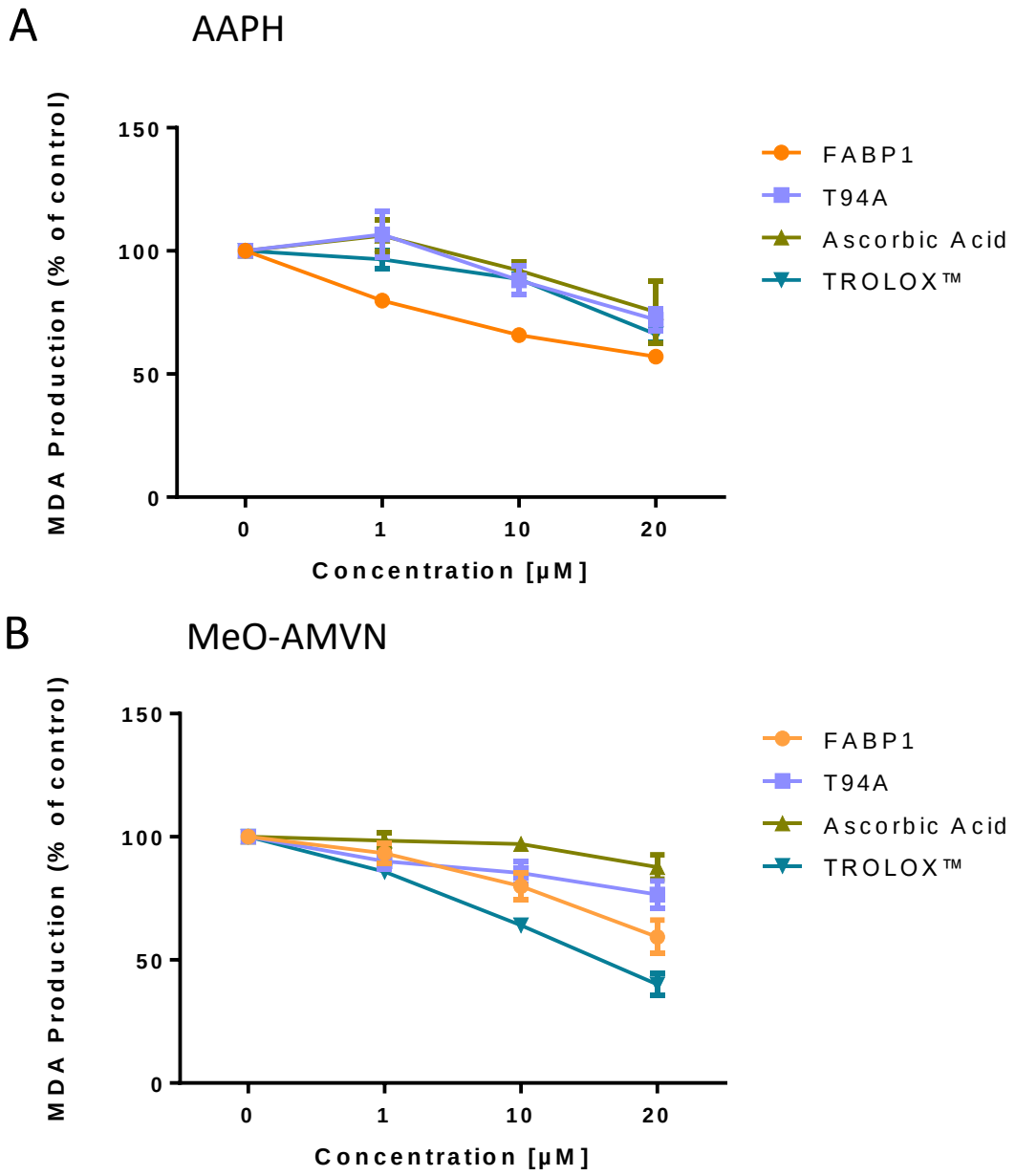

Figure 22: Antioxidants in lipid peroxidation reactions. The effect of FABP1, FABP1 T94A, ascorbic acid, and TROLOX™ on AAPH (A) and MeO-AMVN (B) induced MDA production. LDL was incubated with azo compounds and varying concentrations of FABP1, T94A, ascorbic acid, or TROLOX™ for 90 minutes at 37°C. MDA was measured using the TBARS assay. Values represent mean ± SEM, n = 8, P>0.05.

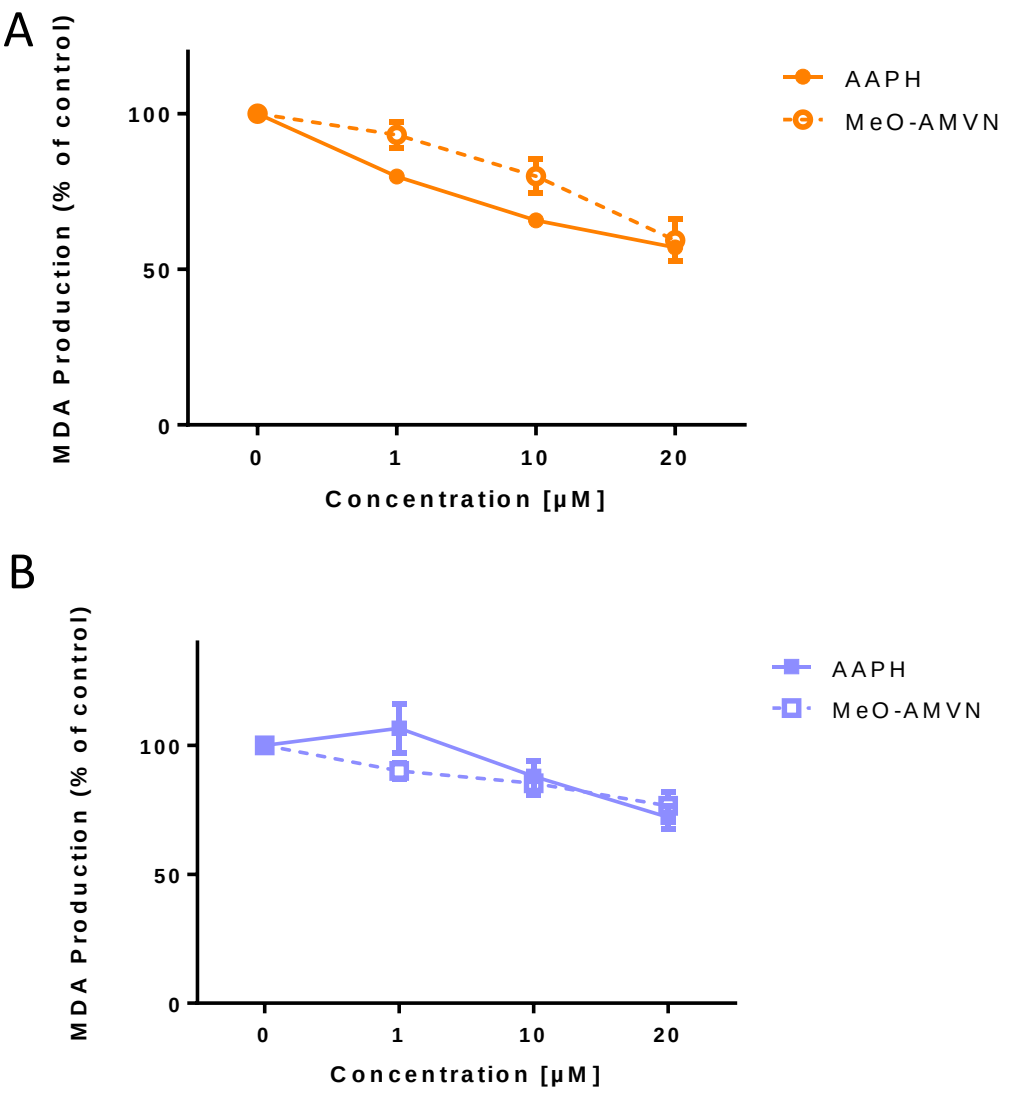

Figure 23: Antioxidant function of FABP1 (A) and T94A (B) in hydrophilic and lipophilic environments. FABP1 T94A concentration (µM) as a function of MDA production (% of control) in an AAPH and MeO-AMVN environment. The data illustrate how both FABP1 and T94A mutation affects the antioxidant function in a hydrophilic versus lipophilic environment. Values represent mean ± SEM, n = 8, P>0.05.

The Influence of Long-Chain Fatty Acid Binding on Recombinant FABP1 T94A's Antioxidant Function

FABP1 contains several antioxidant residues within its binding pocket. Consequently, the binding with ligands such as fatty acids may affect the protein's ability to act as an antioxidant (Yan *et al*. 2009). Yan *et al*. (2009) observed that FABP1 performs as the superior antioxidant when the protein is unbound and was unable to act as well in the presence of fatty acids. In this study the same technique was used to investigate whether FABP1 T94A's function as an antioxidant could be influenced by the binding with fatty acids.

In determining the effects of fatty acid binding, 10 μM purified recombinant proteins were pre-incubated with either 30 μM of palmitate (PA) or alpha-bromo-palmitate (α-Br-PA) for 1 hour at 37°C before being used in the *in* vitro lipid peroxidation reaction and TBARS assay. Keeping the methods similar to Yan *et al.* (2009), long-chain fatty acids used represent reversible binding (PA) or irreversible binding (α-Br-PA). Figure 24 displays results of this assay, showing that FABP1 in all conditions (unbound, bound with PA or bound with α-Br-PA) was able to reduce MDA production in the AAPH and MeO-AMVN free radical generating system. Since the same lipid peroxidation system is used, the control in this case would be the addition of water instead of the antioxidant proteins.

In the AAPH induced condition, unbound FABP1 was able to reduce MDA by 38.9±1.8% of the control whereas FABP1 with PA and α-Br-PA reduced MDA production by 20.2±3.7 and 13.1±1.9% of the control, respectively. When comparing results, there are significant differences between the unbound and bound FABP1 with PA or α-Br-PA (Figure 24A). In the hydrophilic (AAPH) condition, unbound FABP1 had significantly lower amounts of MDA produced compared to that bound with PA and α-Br-PA ($P<0.01$ and $P<0.001$,

respectively). There was no difference in MDA produced when FABP1 was bound to PA or α-Br-PA. While FABP1 in both bound and unbound states was able to reduce MDA production in the induced lipid peroxidation environment by MeO-AMVN, there were no significant difference between the MDA productions (Figure 24A).

As for the FABP1 T94A variant, the addition of the bound and unbound protein reduced MDA production in both AAPH and MeO-AMVN lipid peroxidation systems (Figure 24B). However, only the unbound state was significant (83.2±6.2% in AAPH system and 83.4±5.9% of the control in MeO-AMVN system, $P<0.05$). When comparing the unbound T94A to T94A with PA or with α-Br-PA, MDA was not decreased in both systems. Samples pre-incubated with PA had MDA production of 87.6±2.5% of the control in hydrophilic free radical releasing system and 87.4±1.7% in a lipophilic environment. The MDA production increased to 97.3±1.4% with AAPH derived free radicals when T94A was bound with α-Br-PA but stayed at the same level with MeO-AMVN (87.1±5.5%).

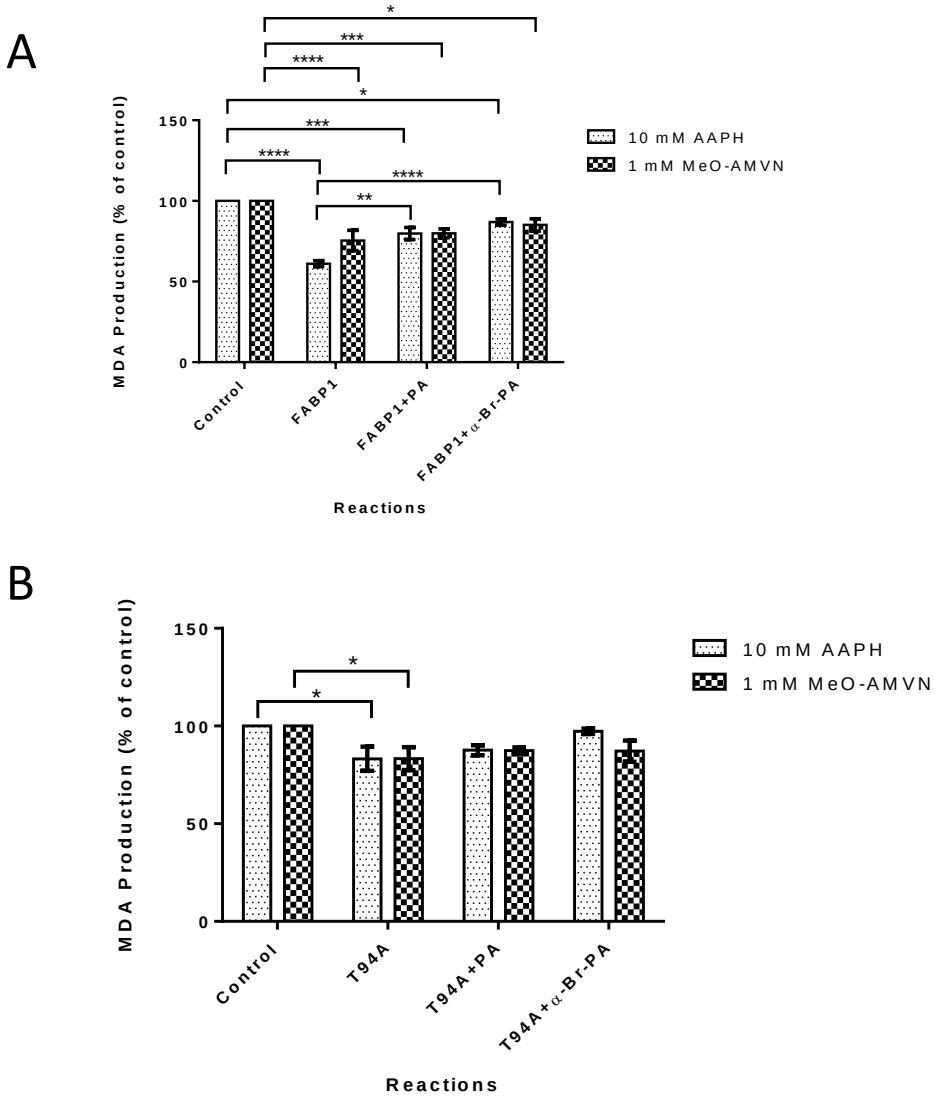

Figure 24: Comparison of the effect of recombinant FABP1 (A) and FABP1 T94A (B) after binding with palmitate (PA) and α-Br-PA on azo compounds AAPH and MeO-AMVN free radical generating system. Recombinant proteins (10 μM) were pre-incubated with PA for 1 hour at 37°C before being used in the lipid peroxidation reactions. MDA levels were measured using the TBARS assay. Control are MDA levels produced in lipid peroxidation reactions without FABP1 or T94A. Values represent mean ± SEM, n = 6, * $p<0.05$, ** $p<0.01$, ***$p<0.001$).

Chapter 4: Discussion

In the current study, recombinant rat FABP1 T94A variant was purified using the GST tag system and *in vitro* studies were used in determining the mutant protein's antioxidant activity. From these results, recombinant rat FABP1 T94A variant acts as an antioxidant and can do so in both simulated *in vitro* hydrophilic and lipophilic environment. There were no significant differences between the performance of the wild type and mutant as antioxidants. This suggests that the T94A substitution does not impact the protein's function as an antioxidant. However, it was found that when T94A was bound to either PA or α-Br-PA, the mutant protein was unable to significantly reduce the generation of MDA which may suggest there is an altered antioxidant function once bound to ligands.

Oxidative stress has been implicated in the pathogenesis of several liver diseases such as NAFLD (Sumida *et al*., 2013; Polimeni 2015), ALD (Minicis and Banner, 2008; Cederbaum *et al*., 2009; Sid *et al*., 2013), Hepatitis C (Koike 2007), and NASH (Morris *et al*., 2013, Sutti *et al*., 2014). The state of oxidative stress is due to an excessive amount of pro-oxidants such ROS and RNS being produced that overwhelms the body's antioxidant system. FABP1, a small (14 kDa) cytosolic protein that is highly ubiquitous in the liver, up to 400 μM in murine and 1000 μM in humans (McArthur *et al*., 1999; Favretto *et al*., 2013), has been shown to act as an antioxidant (Wang *et al*., 2005). FABP1 contains several methionine groups and a single cysteine that was shown to be responsible for the molecular mechanism of the protein's antioxidant capacity (Yan *et al*., 2009). As the name suggests, FABP1 binds LCFA but the protein can also bind other ligands such as peroxisome proliferators (Wolfrum *et al*., 2000), bile acids (Favretto *et al*., 2015), heme (Stewart *et al*., 1996), and endocannabinoids (Schroeder *et al*., 2016). Being capable of functioning as an antioxidant and having the capability to partition fatty acids (free vs

protein-bound) (Anstee *et al*., 2011), FABP1 is considered to be a cytoprotectant (Wang *et al*., 2015). Since FABP1 is speculated to be vital in the redox homeostasis of the liver by being highly present in hepatocytes, binding lipid peroxides, and acting as an antioxidant, the loss of one of these functions can be detrimental. The recently discovered human T94A variant is a SNP that occurs in the coding region of the FABP1 gene (Brouillette *et al*., 2004). Whether this SNP results in altered FAPB1 antioxidant activity was up to now unknown. The T94A SNP has a minor allele frequency of 26-38% and 8.3 ± 1.9% being homozygous in the human population (MAF for 1000 genomes in NCBI dbSNP database; ALFRED database) (Mansego *et al*., 2012).

The FAPB1 T94A variant's reported phenotypes can be inconsistent. An example is the BMIs and waist circumferences where it was initially reported the BMI was lower in carriers of the T94A variant (Brouillette *et al*., 2004), however, it was found to be higher in another study (Peng *et al*., 2012). Differences in the characteristics that the T94A carriers' exhibit may be attributed to the diversity amongst the human population being studied. Moreover, the T94A mutation has been associated with increased LDL cholesterol (Fisher *et al*., 2007), hepatic TAG accumulation (McIntosh *et al*., 2014), higher basal plasma TAG levels (Brouillette *et al*., 2004) and NAFLD (Peng *et al*., 2012). An explanation for these characteristics the polymorphism elicit was hypothesized to be that the T94A mutation results in the total loss of function. However, this was not the case as several studies investigating the mutation have shown that it was an altered function and the T94A variation is not equivalent to ablating the FABP1 gene. For example, it was shown between the wild type and the T94A variant protein, there were no changes in specificity to ligands or changes in the affinity for binding fibrates (Martin *et al*., 2013), steric acid or oleic acid (Huang *et al*., 2014). However, slight changes were seen in the binding affinities between the mutant protein and palmitic acid and linoleic acid (Huang *et al*.,

2014). More differences between the two proteins were reported such as denaturation with temperature (Martin *et al*., 2013) or chemical denaturation (Huang *et al*., 2014), changes in secondary structure in response to binding with ligands (Martin *et al*., 2013;Huang *et al*., 2014), and differences in cholesterol affinity and uptake (Huang *et al*., 2015). While research uncovered various differences between FABP1 and its variant, none have explored the antioxidant function of the mutant. It is important in determining if the T94A mutation is a loss of function mutation with regards to its ability to act as an antioxidant since the pathogenesis of various diseases are linked to oxidative status, the impairment of an essential cytoprotectant such as FABP1 can be deleterious to carriers. Gaining insight on this aspect of the T94A variant is also beneficial to develop new approaches for treating diseases.

Strategies used to purify proteins are based on the differences between the protein of interest and the cell lysate based on their physio-chemical properties. Such methods to separate proteins from mixtures include ion exchange, size exclusion, and hydrophobic interaction chromatography (Cai *et al*., 2012). Current methods combine use of traditional chromatography and affinity tags such as polyhistidine (Zhang *et al*., 2013) and GST (Oyama *et al*., 2005). Since rat cDNA ligated in a pGEX-6P-2 vector in *E. coli* cells was used from a previous study (Yan *et al*., 2009), the purification of FABP1 followed similar steps outlined by the previous researchers. To obtain the T94A variant, site directed mutagenesis was used to induce a mutation in the rat cDNA. With the use of pGEX-6P-2 as a vector the affinity tag attached to FABP1 was GST. GST is a protein tag having the size of 26 kDa and provides a simple and fast method to separate the fusion protein. In the current study, the fusion protein was the GST tag with the FABP1 or the T94A variant. This fusion protein was isolated from the bacterial sonicate using the GST

tag's affinity for the immobilized glutathione on a column and eventually eluted using reduced glutathione.

The GST tag has been shown to protect the fusion protein from intracellular proteolysis (Young *et al*., 2012) and aids in keeping the protein soluble (Malhotra 2009). Results from the current study reveal no presence of insoluble aggregates as seen in lanes 7 and 8 of Figure 17A where the fusion protein is evident at the 40 kDa band. Yan *et al*. (2009) also reported no issues with insoluble aggregates. While there are many methods to isolate the targeted recombinant protein from the cell lysate, the GST affinity tag system has been shown to be reliable (Yan *et al*., 2009). The GST tag system can achieve a pure sample (Figure 17A last two lanes) and can produce 40-50 mg/L of bacterial culture (with the current study) and even up to 50-60 mg per 500 mL culture as reported by Yan *et al*. (2009). Studies using different strategies to purify recombinant FABPs reported yields of 30 mg/L of culture using traditional chromatography (He *et al*., 2007) and 25 mg for single liter of culture (Wang *et al*., 2017) using the HST tag system. It is also worth mentioning that while the GST system provides high yields, the removal of the GST tag leaves an infusion linker at the N-terminal of the protein. This was also seen in Yan *et al*. (2009) study where the linker was identified as GPLGSLAT sequence. In the current study, the infusion linker left at the N-terminal was GPLGSIAT increasing the proteins molecular weight to 14968.0 and 14938.0 Da for FABP1 and T94A respectively (Figure 18) versus the calculated molecular weights of 14272.5 and 14242.5 Da. These extra sequences were speculated to prevent protein degradation (Carr *et al*., 1999), however, the protein fragment is a natural drawback from using PreScission Protease to remove the affinity tag. PreScission Protease is a Rhinovirus 14 3C protease that recognizes the LEVLFQ↓GP sequence cleaving before the glycine and proline leaving dipeptide in front of the N-terminal (Waugh 2011). Further, the

purification reported by Yan *et al*. (2009) revealed that purified FABP1 had the 69th amino acid, cysteine, glutathionylated attributing to a total weight of 15275.9 Da whereas the current study observed no additional weight. This discrepancy may be possibly due to changes in the protocol of the purification step. The current study used GSTrap columns to separate the fusion protein from the protein mix while the previous study used Glutathione Sepharose 4B beads. Nevertheless, both wild type FABP1 and the T94A variant were successfully purified with little to no contaminants using the GST tag system (Figure 17A) and the protein yield was sufficient for downstream studies.

In determining if the FABP1 T94A variant possess the antioxidant function, the DCF fluorescence assay was used. Explained in the preceding section, FABP1 is believed to be a formidable cytoprotectant. Cysteine and methionine both contain sulfur atoms where its electronegativity makes them highly susceptible to oxidation. Not only are these residues easily oxidized they take part in redox cycling reactions that regenerate these residues. Solvent accessible methionine and cysteine residues can be oxidized by ROS into methionine sulfoxide and sulfenic acid/sulfinic acid/sulfonic acid, respectively. These residues are reduced back by methionine sulfoxide reductase (Levine *et al*., 1996) and thioredoxin (Jan *et al*., 2014). FABP1 has seven methionine and one cysteine residue that can scavenge ROS making the protein a compelling case to investigate its antioxidant capacity. This aspect of FABP1 was demonstrated with Chang cells stably transfected with FABP1 having lower concentrations of ROS than those that were not transfected (Wang *et al*., 2005). The manipulation of FABP1 levels using pharmaceuticals, clofibrate and dexamethasone, added insight FABP1 acting as an endogenous cytoprotectant in models of H_2O_2 incubation or hypoxia-reoxygenation (Rajaraman *et al*., 2007). Furthermore, FABP1 retains this function in an *in vivo* study using bile-duct ligated model of

cholestasis where bile-duct ligated rats treated with clofibrate restored FABP1 levels (Wang *et al*., 2007). Additionally, clofibrate was found to increase the gene transcription of FABP1 (Yan *et al*., 2010), FABP1 (-/-) mice fed ethanol had higher levels of oxidative stress exhibiting increased lipid peroxidation products such as 4-hydroxynonenal and MDA (Smathers *et al*., 2013), and FABP1 acts as an hepatoprotectant in an *in vitro* model of acetaminophen overdose (Gong *et al*., 2014). Recently, FABP1 has been shown to act as an antioxidant in an *in vitro* cell model of NAFLD using a 2:1 proportion of palmitic acid to oleic acid (Chen *et al*., 2017).

In the present study, it was determined that the recombinant rat FABP1 T94A variant can scavenge ROS as seen in Figure 20. DCFH reacts with ROS to produce the fluorescence DCF, which can be measured at an excitation at 485 and emission at 590 nm. Hydrogen peroxide in the reaction was not enough to produce DCF since the DCFH probe has poor sensitivity to H_2O_2 (Wardman 2007). Instead the ROS generated in the reactions was the hydroxyl radical using the Fenton reaction where H_2O_2 reacts with ferrous perchlorate to yield the ROS (Halliwell and Whiteman, 2004). The decrease in DCF fluorescence suggested that FABP1 T94A variant was able to scavenge the hydroxyl radical decreasing the availability of ROS to react with the DCFH probe (Figure 10). When comparing FABP1 to the FABP1 T94A variant, there were no significant differences between the ability to reduce DCF fluorescence which potentially means that both proteins are able to scavenge the hydroxyl radical equally. The ability of FABP1's to reduce DCF fluorescence in the current study is consistent with Yan *et al.* (2009) despite the lower range of concentrations used in the present study. This indicated that protein purification was performed correctly since there were no changes in function.

To further assess the capabilities of FABP1 T94A as an antioxidant, the protein was subjected to lipid peroxidation reactions simulated in two environments. AMVN and MeO-

AMVN are azo compounds that thermally decompose into free radicals. AMVN produces free radicals in the hydrophilic environment while MeO-AMVN produces free radicals in the lipophilic environment. LDL is included in these lipid peroxidation reactions to provide lipids for the free radicals to attack resulting in lipid peroxides such as MDA. These lipid peroxidation products are highly reactive forming adducts with biologically important macromolecules. Hence the TBARS assay was used to measure the generated lipid peroxidation products. A previous study has demonstrated that FABP1 was an effective antioxidant in both lipophilic and hydrophilic milieus (Yan *et al*., 2009). From Figure 22, the addition of FABP1 T94A into the oxidation reactions produced lower amounts of MDA as the concentration of the protein increased. This indicates that the mutant variant can act as both a hydrophilic and lipophilic antioxidant preventing the formation of MDA. Comparing the performance of the mutant variant to the wild type, significant difference was found at 1 μM and 10 μM but no differences were seen with 20 μM in the AAPH system (Figure 22A). The result may mean that at lower concentrations the T94A variant may not have as much accessible antioxidant moieties as the wild type. However, at higher concentrations the variant may perform similarly as the wild type (at 20 μM). Since FABP1's concentration in human hepatocytes may be as high as 1000 μM (McArthur *et al*., 1999; Favretto *et al*., 2013), the difference between the mutated and non-mutated forms may be negligible assuming that at concentrations higher than 20 μM, the proteins behave similarly in a hydrophilic environment.

When examining the proteins in the MeO-AMVN system, there were no significant differences between the two (Figure 22B). This suggest that the T94A mutation did not alter the protein structure in way that inhibits the antioxidant moieties from scavenging ROS in a lipophilic environment. Since there are no significant differences in T94A variant's

effectiveness as an antioxidant it can be speculated that the same amino acid residues as FABP1 are responsible (Yan *et al*., 2009), however, further studies are needed to confirm this. Comparing the action of FABP1 in this study with Yan *et al*. (2009) in both cases the purified recombinant proteins are able to decrease ROS. As commented on earlier, the protein in the present study did not have a glutathionylated cysteine residue but because no increase in antioxidant activity was observed this suggest that the cysteine residue may not be solvent accessible and might be buried within the protein's binding cavity.

FABP1's antioxidant function was attenuated when bound with either PA or α-Br-PA in both AAPH and MeO-AMVN lipid peroxidation reactions but was still able to significantly decrease MDA production (Figure 24). These results are consistent with Yan *et al*. (2009) where a similar trend is seen. Contrast with this result is with the T94A variant where there were no significant difference found between the control and the mutant variant bound with either PA or α-Br-PA (Figure 24B). The result potentially indicate that when the mutant variant binds to ligands the protein is unable to scavenge ROS. The antioxidant amino acids of the FABP1 T94A may have become unavailable when ligands are bound. Studies have shown no change in ligand specificity and affinity to some ligands (Martin *et al*., 2013 and Huang *et al*., 2014) which implies that the mutation does not lose function. Yet these studies have shown that despite not losing functionality, the protein's function is altered specifically with regards to the protein's secondary structure response when bound to ligands influencing the downstream interaction with PPARα (Martin *et al*., 2013). Consistent with these findings, the present study have found that there were no loss in function in antioxidant activity but the results seen in Figure 24 imply that ligands can influence the T94A variant differently from FABP1. Huang *et al.* (2014) reported T94A having a lower binding affinity with palmitic and linoleic acid which may illustrate that

T94A variant could be more readily available to act as an antioxidant. This was not observed as the antioxidant ability was hindered when FABP1 T94A was bound to both FAs. Secondary structural changes in response to LCFAs binding to the T94A variant is a possible reason for the weakened antioxidant response.

NAFLD is one of the most common liver dysfunction around the world (Loomba *et al*., 2013). NAFLD comprises of a spectrum of conditions from HCC, cirrhosis, steatosis, or NASH with or without fibrosis. NAFLD can be defined as having hepatic triglyceride (TG) without the excessive consumption of alcohol. Considered as the hepatic manifestation of metabolic syndrome (Chalasani *et al*., 2012) the most frequent comorbidities associated with NAFLD are obesity (Moore 2010), type-2 diabetes mellitus (T2DM) (Ismail 2011), cardiovascular disease (CVD) (Hamaguchi *et al*., 2007), and hyperlipidemia (Browning *et al*., 2004). One-fifth (20%) of NAFLD patients are categorized as NASH having hepatocellular injury and lobular inflammation (Angulo 2012). Considered a complex disease, the understanding of NAFLD and NASH pathogenesis is still incomplete where several factors such as insulin resistance, mitochondrial activity, intestinal microbiota, environmental factors (life style choices and nutrition) and genetics influence the disease process (Haas *et al*., 2016). The traditional two hit hypothesis for the pathophysiologic model of NAFLD describes the first hit as the development of steatosis closely associated with insulin resistance while the second hit is the development to NASH due to oxidative stress and lipid peroxidation (Pagadala and McCullough, 2012). FABP1 T94A variant has been associated with NAFLD (Peng *et al*., 2012 and Tian *et al*., 2015). Studies have investigated the variant's characteristics to provide possible explanation for the association between FABP1 T94A and NAFLD. Transfected Chang cells with FABP1 T94A had lower uptake of radiolabelled palmitic acid (Gao *et al*., 2010) and human hepatocytes expressing

FABP1 had increased uptake of radiolabelled and fluorescent steric acid than the T94A counterpart (McIntosh *et al*., 2014). Moreover, the binding affinity to cholesterol was higher with T94A variant than FABP1 (Huang *et al*., 2014). These studies give insight for why carriers of FABP1 T94A may be more susceptible to NAFLD because these differences between the wild type and mutant may cause the development of steatosis, the first hit. The SNP's impact could go beyond the first hit and into the second as it was established that FABP1 acts as an antioxidant reducing oxidative stress and lipid peroxidation products. If the T94A variant loses its function as an antioxidant then the SNP contributes to not only the first hit but also the second hit for NAFLD. In the current study, it was found that FABP1 T94A variant still maintains its antioxidant property therefore, does not necessarily contribute to the second hit of NAFLD. Interestingly when LCFAs bind to FABP1 T94A, the antioxidant property was diminished suggesting a possible role of the T94A variant in the second hit in the pathogenesis of NAFLD.

Chapter 5: Conclusion

With the discovery of a SNP in the human FABP1 gene, many studies were interested in illustrating differences in phenotype of the FABP1 T94A variant since the mutation is considered common having a minor allele frequency of between 26-38%. Showing the impact the variant has on human health is important as the variant is one of the most dominant polymorphisms within the family of intracellular fatty acid binding proteins. Studies have investigated the difference between the proteins from the ligand binding aspect but none have looked at variant's antioxidant function. The present study objective was in determining whether the mutation of FABP1 would have a loss of function in its antioxidant property.

This study used *E. coli* cells containing pGex-6P-2 vector with rat FABP1 cDNA inserted into the plasmid to generate rat T94A cDNA using site directed mutagenesis. The induction of the mutation was successful as transformed colonies were able to grow on ampicillin treated agar plates and DNA sequencing of the plasmid confirmed the substitution. Recombinant rat T94A was expressed and purified using the GST affinity tag system. To determine if the correct protein was purified SDS-PAGE, western blot, and LC-MS was used.

The mutant variant was determined to scavenge ROS such as the hydroxyl radical in the DCF fluorescence assay. To further evaluate the protein's effectiveness as an antioxidant, the variant was added into lipid peroxidation reactions. It was found that T94A was able to suppress the production of MDA, a lipid peroxidation product in simulated hydrophilic and lipophilic environments. The study also found that when FAs bind to the T94A variant, the protein's ability as an antioxidant was somewhat hindered. The present studies have filled a gap in knowledge of the FABP1 T94A. Future studies should expand upon the molecular mechanism of the FABP1 T94A's antioxidant property and compare the data with FABP1. Future work may also investigate differences in ligand binding characteristics that have not been investigated and determine whether these ligands influence the solvent accessibility of the antioxidant amino acids.

References

Albano E, Mottaran E, Vidali M, Reale E, Saksena S, Occhino G, et al. Immune response towards lipid peroxidation products as a predictor of progression of non-alcoholic fatty liver disease to advanced fibrosis. Gut. 2005;54(7):987–93.

Angulo P. Nonalcoholic fatty liver disease. N Engl J Med. 2002;346(16):1221–31.

Anstee Q, Daly A, Day C. Genetic modifiers of non-alcoholic fatty liver disease progression. Biochimica Et Biophysica Acta Bba - Mol Basis Dis. 2011;1812(11):1557–66.

Avery M, Huang H, Storey S, Landrock K, Landrock D, Petrescu A, et al. Human FABP1 T94A variant impacts fatty acid metabolism and PPAR-α activation in cultured human female hepatocytes. Am J Physiology - Gastrointest Liver Physiology. 2014;307(2):G164–76.

Bailey SM, Cunningham CC. Contribution of mitochondria to oxidative stress associated with alcoholic liver disease. Free Radic Biol Med. 2002;32(1):11–6.

Banaszak L, Winter N, Xu Z, Bernlohr DA, Cowan S, Jones AT. Lipid-Binding Proteins: A Family of Fatty Acid and Retinoid Transport Proteins. Advances in Protein Chemistry. 1994;45:89–151.

Bass NM. The Cellular Fatty Acid Binding Proteins: Aspects of Structure, Regulation, and Function. International Review of Cytology. 1988;111:143–84.

Betts MJ, Russell RB. Amino Acid Properties and Conseaquences of Substitutions. In: Bioinformatics for Geneticists. 2003. p. 289–316.

Birnboim H, Doly J. A rapid alkaline extraction procedure for screening recombinant plasmid DNA. Nucleic Acids Res. 1979;7(6):1513–23.

Boelsterli UA. Diclofenac-induced liver injury: a paradigm of idiosyncratic drug toxicity. Toxicology and Applied Pharmacology. 2003;192(3):307–22.

Boyer TD, Manns MP, Sanyal AJ, Zakim D. Zakim and Boyer's hepatology : a textbook of liver disease. 6th ed.. Philadelphia, PA: Saunders/Elsevier; 2012. xiv+1314 p.

Brenner D, Kisseleva T, Scholten D, Paik Y, Iwaisako K, Inokuchi S, et al. Origin of myofibroblasts in liver fibrosis. Fibrogenesis Tissue Repair. 2012;5(S1):1–4.

Brouillette C, Bossé Y, Pérusse L, Gaudet D, Vohl M-C. Effect of liver fatty acid binding protein (FABP) T94A missense mutation on plasma lipoprotein responsiveness to treatment with fenofibrate. Journal of Human Genetics. 0;49(8):424–32.

Browning J, Szczepaniak L, Dobbins R, Nuremberg P, Horton J, Cohen J, et al. Prevalence of hepatic steatosis in an urban population in the United States: Impact of ethnicity. Hepatology. 2004;40(6):1387–95.

Buss H, Chan T, Sluis K, Domigan N, Winterbourn C. Protein Carbonyl Measurement by a Sensitive ELISA Method. Free Radical Bio Med. 1997;23(3):361–6.

Cai J, Lücke C, Chen Z, Qiao Y, Klimtchuk E, Hamilton JA. Solution Structure and Backbone Dynamics of Human Liver Fatty Acid Binding Protein: Fatty Acid Binding Revisited. Biophys J. 2012;102(11):2585–94.

Carr S, Miller J, Leary SE., Bennett A., Ho A, Williamson E. Expression of a recombinant form of the V antigen of Yersinia pestis, using three different expression systems. Vaccine. 1999;18(1-2):153–9.

Carter P. Site-directed mutagenesis. Biochem J. 1986;237(1):1–7.

Cederbaum AI, Lu Y, Wu D. Role of oxidative stress in alcohol-induced liver injury. Arch Toxicol. 2009;83(6):519–48.

Chalasani N, Younossi Z, Lavine JE, Diehl AM, Brunt EM, Cusi K, et al. The diagnosis and management of non-alcoholic fatty liver disease: practice Guideline by the American Association for the Study of Liver Diseases, American College of Gastroenterology, and the American Gastroenterological Association. Hepatology. 2012;55(6):2005–23.

Chen S, Tuinen P, Ledbetter D, Smith L, Chan L. Human liver fatty acid binding protein gene is located on chromosome 2. Somat Cell Molec Gen. 1986;12(3):303–6.

Chen Y, Li W, Yuewen G, Guqi W, Frank B. Clofibrate Attenuates ROS Production by Lipid Overload in Cultured Rat Hepatoma Cells. J Pharm Pharm Sci. 2017;20:239–51.

Chmurzyńska A. The multigene family of fatty acid-binding proteins (FABPs): Function, structure and polymorphism. J Appl Genet. 2006;47(1):39–48.

Coe N, Bernlohr D. Physiological properties and functions of intracellular fatty acid-binding proteins. Biochimica Et Biophysica Acta Bba - Lipids Lipid Metabolism. 1998;1391(3):287–306.

Costa S, Almeida A, Castro A, Domingues L. Fusion tags for protein solubility, purification and immunogenicity in Escherichia coli: the novel Fh8 system. Front Microbiol. 2014;5:63.

Drüeke T, Véronique W-S, Massy Z, Béatrice D-L, Guerin A, Marchais S, et al. Iron Therapy, Advanced Oxidation Protein Products, and Carotid Artery Intima-Media Thickness in End-Stage Renal Disease. Circulation. 2002;106(17):2212–7.

Favretto F, Assfalg M, Gallo M, Cicero D, Mariapina D, Molinari H. Ligand Binding Promiscuity of Human Liver Fatty Acid Binding Protein: Structural and Dynamic Insights from an Interaction Study with Glycocholate and Oleate. Chembiochem. 2013;14(14):1807–19.

Favretto F, Santambrogio C, Mariapina D, Molinari H, Grandori R, Assfalg M. Bile salt recognition by human liver fatty acid binding protein. Febs J. 2015;282(7):1271–88.

Feng Y, Wang N, Ye X, Li H, Feng Y, Cheung F, et al. Hepatoprotective effect and its possible mechanism of Coptidis rhizoma aqueous extract on carbon tetrachloride-induced chronic liver hepatotoxicity in rats. J Ethnopharmacol. 2011;138(3):683–90.

Fisher E, Weikert C, Klapper M, Lindner I, Möhlig M, Spranger J, et al. L-FABP T94A is associated with fasting triglycerides and LDL-cholesterol in women. Molecular Genetics and Metabolism. 2007;91(3):278–84.

Furuhashi M, Hotamisligil GS. Fatty acid-binding proteins: role in metabolic diseases and potential as drug targets. Nature Reviews Drug Discovery. 2008;7(6):489–503.

Gao N, Qu X, Yan J, Huang Q, Yuan H-Y, Ouyang D-S. L-FABP T94A decreased fatty acid uptake and altered hepatic triglyceride and cholesterol accumulation in Chang liver cells stably transfected with L-FABP. Molecular and Cellular Biochemistry. 2010;345(1-2):207–14.

Gerswhin Me, Vierling JM, Manns MP. Liver Immunology. Humana Press; 2007.

Gong Y, Gong Y, Wang G, Gong Y, Burczynski F. Regulation of liver fatty acid binding protein expression by clofibrate in hepatoma cells. Biochem Cell Biology. 2010;88(6):957–67.

Gong Y, Wang G, Gong Y, Yan J, Chen Y, Burczynski F. Hepatoprotective role of liver fatty acid binding protein in acetaminophen induced toxicity. Bmc Gastroenterol. 2014;14(1):1–7.

Gusdon AM, Song K-XX, Qu S. Nonalcoholic Fatty liver disease: pathogenesis and therapeutics from a mitochondria-centric perspective. Oxid Med Cell Longev. 2014;2014:637027.

Haas JT, Francque S, Staels B. Pathophysiology and Mechanisms of Nonalcoholic Fatty Liver Disease. Annu Rev Physiol. 2016;78(1):181–205.

Halliwell B, Chirico S. Lipid peroxidation: its mechanism, measurement, and significance. The American Journal of Clinical Nutrition. 1993;57(5 Suppl):715S – 724S; discussion 724S – 725S.

Halliwell B, Whiteman M. Measuring reactive species and oxidative damage in vivo and in cell culture: how should you do it and what do the results mean? Br J Pharmacol. 2004;142(2):231–55.

Halina C-L. Oxidative stress as a crucial factor in liver diseases. World J Gastroentero. 2014;20(25):8082.

Hamaguchi M, Kojima T, Takeda N, Nagata C, Takeda J, Sarui H, et al. Nonalcoholic fatty liver disease is a novel predictor of cardiovascular disease. World J Gastroenterol. 2007;13(10):1579–84.

Handler J, Thurman R. Redox interactions between catalase and alcohol dehydrogenase pathways of ethanol metabolism in the perfused rat liver. J Biol Chem. 1990;265(3):1510–5.

Hanhoff T, Lücke C, Spener F. Insights into binding of fatty acids by fatty acid binding proteins. Molecular and Cellular Biochemistry. 2002;239(1-2):45–54.

He F, Zuo L. Redox Roles of Reactive Oxygen Species in Cardiovascular Diseases. Int J Mol Sci. 2015;16(11):27770–80.

He Y, Yang X, Wang H, Estephan R, Francis F, Kodukula S, et al. Solution-State Molecular Structure of Apo and Oleate-Liganded Liver Fatty Acid-Binding Protein†. Biochemistry-us. 2007;46(44):12543–56.

Hirata Y, Yamamoto E, Tokitsu T, Fujisue K, Kurokawa H, Sugamura K, et al. The Pivotal Role of a Novel Biomarker of Reactive Oxygen Species in Chronic Kidney Disease. Medicine. 2015;94(25):e1040.

Huang H, L M Avery, Landrock KK, Landrock D, Storey SM, Martin GG, et al. Human FABP1 T94A variant enhances cholesterol uptake. Biochimica Et Biophysica Acta. 2015;1851(7):946–55.

Huang H, L M Avery, Martin GG, Landrock KK, Landrock D, Gupta S, et al. Structural and functional interaction of fatty acids with human liver fatty acid-binding protein (L-FABP) T94A variant. The FEBS journal. 2014;281(9):2266–83.

Huang H, Starodub O, Avery M, Kier A, Schroeder F. Liver Fatty Acid-binding Protein Targets Fatty Acids to the Nucleus REAL TIME CONFOCAL AND MULTIPHOTON FLUORESCENCE IMAGING IN LIVING CELLS. J Biol Chem. 2002;277(32):29139–51.

Huang W, Zhang X, Chen W. Role of oxidative stress in Alzheimer's disease (Review). Biomed Reports. 2016;

Ismail MH. Nonalcoholic fatty liver disease and type 2 diabetes mellitus: the hidden epidemic. Am J Med Sci. 2011;341(6):485–92.

Jaeschke H. Reactive oxygen and mechanisms of inflammatory liver injury: Present concepts. Journal of Gastroenterology and Hepatology. 2011;26 Suppl 1:173–9.

Jan Y-H, Heck DE, Dragomir A-C, Gardner C, Laskin D, Laskin J. Acetaminophen Reactive Intermediates Target Hepatic Thioredoxin Reductase. Chem Res Toxicol. 2014;27(5):882–94.

Kathirvel E, Chen P, Morgan K, French S, Morgan T. Oxidative stress and regulation of anti-oxidant enzymes in cytochrome P4502E1 transgenic mouse model of non-alcoholic fatty liver. J Gastroen Hepatol. 2010;25(6):1136–43.

Kawashima Y, Nakagawa S, Tachibana Y, Kozuka H. Effects of peroxisome proliferators on fatty acid-binding protein in rat liver. Biochim Biophys Acta. 1983;754(1):21–7.

Kobayashi E, Suzuki T, Yamamoto M. Roles Nrf2 Plays in Myeloid Cells and Related Disorders. Oxid Med Cell Longev. 2013;2013:1–7.

Koike K. Pathogenesis of HCV-associated HCC: Dual-pass carcinogenesis through activation of oxidative stress and intracellular signaling. Hepatol Res. 2007;37(s2):S115–20.

Konishi M, Iwasa M, Araki J, Kobayashi Y, Katsuki A, Sumida Y, et al. Increased lipid peroxidation in patients with non-alcoholic fatty liver disease and chronic hepatitis C as measured by the plasma level of 8-isoprostane. Journal of Gastroenterology and Hepatology. 2006;21(12):1821–5.

Lee D-HH, R O Timothy, Pfeifer GP. Oxidative DNA damage induced by copper and hydrogen peroxide promotes CG–{\textgreater}TT tandem mutations at methylated CpG dinucleotides in nucleotide excision repair-deficient cells. Nucleic Acids Res. 2002;30(16):3566–73.

Levi A, Arias I. Two hepatic cytoplasmic protein fractions, Y and Z, and their possible role in the hepatic uptake of bilirubin, sulfobromophthalein, and other anions. J Clin Invest. 1969;48(11):2156–67.

Levine R, Moskovitz J, Stadtman E. Oxidation of methionine in proteins: roles in antioxidant defense and cellular regulation. IUBMB life. 2000;50(4-5):301–7.

Levine R, Stadtman E. Oxidative modification of proteins during aging. Exp Gerontol. 2001;36(9):1495–502.

Levine R, Berlett B, Moskovitz J, Mosoni L, Stadtman E. Methionine residues may protect proteins from critical oxidative damage. Mech Ageing Dev. 1999;107(3):323–32.

Levine RL, Mosoni L, Berlett BS, Stadtman ER. Methionine residues as endogenous antioxidants in proteins. Proc National Acad Sci. 1996;93(26):15036–40.

Li H, Horke S, Förstermann U. Vascular oxidative stress, nitric oxide and atherosclerosis. Atherosclerosis. 2014;237(1):208–19.

Liochev S. Reactive oxygen species and the free radical theory of aging. Free Radical Bio Med. 2013; 60:1–4.

Lobo V, Patil A, Phatak A, Chandra N. Free radicals, antioxidants and functional foods: Impact on human health. Pharmacognosy Reviews. 2010;4(8):118–26.

Loomba R, Wolfson T, Ang B, Hooker J, Behling C, Peterson M, et al. Magnetic resonance elastography predicts advanced fibrosis in patients with nonalcoholic fatty liver disease: A prospective study. Hepatology. 2014;60(6):1920–8.

Loureiro A, Mascio P, Gomes O, Medeiros M. trans,trans-2,4-Decadienal-Induced 1,N2-Etheno-2‘-deoxyguanosine Adduct Formation. Chem Res Toxicol. 2000;13(7):601–9.

Malhotra A. Tagging for protein expression. Meth Enzymol. 2009;463:239–58.

Mansego M, Martínez F, Maria M-L, Zabena C, Rojo G, Morcillo S, et al. Common Variants of the Liver Fatty Acid Binding Protein Gene Influence the Risk of Type 2 Diabetes and Insulin Resistance in Spanish Population. Plos One. 2012;7(3):e31853.

Marnett L. Oxyradicals and DNA damage. Carcinogenesis. 2000;21(3):361–70.

Martin G, Avery M, Huang H, Gupta S, Atshaves B, Landrock K, et al. The Human Liver Fatty Acid Binding Protein T94A Variant Alters the Structure, Stability, and Interaction with Fibrates. Biochemistry-us. 2013;52(51):9347–57.

Minicis S, Brenner D. Oxidative stress in alcoholic liver disease: Role of NADPH oxidase complex. J Gastroen Hepatol. 2008;23(s1):S98–103.

MJ M, Atshaves B, Frolov A, Foxworth W, Kier A, Schroeder F. Cellular uptake and intracellular trafficking of long chain fatty acids. J Lipid Res. 1999;40(8):1371–83.

Mohsen M, Iravani M, Spencer J, Rose S, Fahim A, Motawi T, et al. Age-associated changes in protein oxidation and proteasome activities in rat brain: Modulation by antioxidants. Biochem Bioph Res Co. 2005;336(2):386–91.

Moore BJ. Non-alcoholic fatty liver disease: the hepatic consequence of obesity and the metabolic syndrome. P Nutr Soc. 2010;69(2):211–20.

Morris E, Fletcher J, Thyfault J, Rector R. The role of angiotensin II in nonalcoholic steatohepatitis. Mol Cell Endocrinol. 2013;378(1-2):29–40.

Moskovitz J, Jenkins N, Gilbert D, Copeland N, Jursky F, Weissbach H, et al. Chromosomal localization of the mammalian peptide-methionine sulfoxide reductase gene and its differential expression in various tissues. Proc National Acad Sci. 1996;93(8):3205–8.

Nakagawa S, Kawashima Y, Hirose A, Kozuka H. Regulation of hepatic level of fatty-acid-binding protein by hormones and clofibric acid in the rat. Biochem J. 1994;297(3):581–4.

Ockner R, Manning J, Poppenhausen R, Ho W. A binding protein for fatty acids in cytosol of intestinal mucosa, liver, myocardium, and other tissues. Science. 1972;177(4043):56–8.

Odani S, Namba Y, Ishii A, Ono T, Fujii H. Disulfide bonds in rat cutaneous fatty acid-binding protein. J Biochem. 2000;128(3):355–61.

Oyama Y, Takeda T, Hama H, Tanuma A, Iino N, Sato K, et al. Evidence for megalin-mediated proximal tubular uptake of L-FABP, a carrier of potentially nephrotoxic molecules. Lab Invest. 2005;85(4):522–31.

Pagadala MR, J M Arthur. Non-alcoholic fatty liver disease and obesity: not all about body mass index. Am J Gastroenterol. 2012;107(12):1859–61.

Pamplona R. Membrane phospholipids, lipoxidative damage and molecular integrity: A causal role in aging and longevity. Biochimica et Biophysica Acta (BBA) - Bioenergetics. 2008;1777(10):1249–62.

Parola M, Robino G. Oxidative stress-related molecules and liver fibrosis. J Hepatol. 2001;35(2):297–306.

Peng X-E, Wu Y-L, Lu Q-Q, Hu Z-J, Lin X. Two genetic variants in FABP1 and susceptibility to non-alcohol fatty liver disease in a Chinese population. Gene. 2012;500(1):54–8.

Polimeni L. Oxidative stress: New insights on the association of non-alcoholic fatty liver disease and atherosclerosis. World J Hepatology. 2015;7(10):1325.

Rajaraman G, Burczynski F. Effect of dexamethasone, 2-bromopalmitate and clofibrate on L-FABP mediated hepatoma proliferation. J Pharm Pharmacol. 2004;56(9):1155–61.

Rajaraman G, Wang G, Yan J, Jiang P, Gong Y, Burczynski F. Role of cytosolic liver fatty acid binding protein in hepatocellular oxidative stress: effect of dexamethasone and clofibrate treatment. Mol Cell Biochem. 2007;295(1-2):27–34.

Roberts R. How restriction enzymes became the workhorses of molecular biology. Proc National Acad Sci. 2005;102(17):5905–8.

Robitaille J, Brouillette C, Lemieux S, Pérusse L, Gaudet D, Vohl M. Plasma concentrations of apolipoprotein B are modulated by a gene–diet interaction effect between the LFABP T94A polymorphism and dietary fat intake in French-Canadian men. Molecular Genetics and Metabolism. 2004;82(4):296–303.

Rolf B, Elke O-K, Börchers T, F\a ergeman N, Knudsen J, Lezius A, et al. Analysis of the ligand binding properties of recombinant bovine liver-type fatty acid binding protein. Biochimica Et Biophysica Acta Bba - Lipids Lipid Metabolism. 1995;1259(3):245–53.

Sacchettini J, Gordon J, Banaszak L. The structure of crystalline Escherichia coli-derived rat intestinal fatty acid-binding protein at 2.5-A resolution. J Biol Chem. 1988;263(12):5815–9.

Sattar N, Forrest E, Preiss D. Non-alcoholic fatty liver disease. Bmj. 2014;349(sep19 15):g4596.

Schachtrup C, Emmler T, Bleck B, Sandqvist A, Spener F. Functional analysis of peroxisome-proliferator-responsive element motifs in genes of fatty acid-binding proteins. Biochem J. 2004;382(Pt 1):239.

Schlezinger JJ, Struntz WD, Goldstone JV, Stegeman JJ. Uncoupling of cytochrome P450 1A and stimulation of reactive oxygen species production by co-planar polychlorinated biphenyl congeners. Aquatic Toxicology (Amsterdam, Netherlands). 2006;77(4):422–32.

Schroeder F, L M Avery, Martin GG, Huang H, Landrock D, Chung S, et al. Fatty Acid Binding Protein-1 (FABP1) and the Human FABP1 T94A Variant: Roles in the Endocannabinoid System and Dyslipidemias. Lipids. 2016;51(6):655–76.

Sharma A, Sharma A. Fatty Acid Induced Remodeling within the Human Liver Fatty Acid-binding Protein. J Biol Chem. 2011;286(36):31924–8.

Sid B, Verrax J, Calderon P. Role of oxidative stress in the pathogenesis of alcohol-induced liver disease. Free Radical Res. 2013;47(11):894–904.

Singal AK, Jampana SC, Weinman SA. Antioxidants as therapeutic agents for liver disease. Liver Int. 2011;31(10):1432–48.

Smathers R, Galligan J, Shearn C, Fritz K, Mercer K, Ronis M, et al. Susceptibility of L-FABP−/− mice to oxidative stress in early-stage alcoholic liver. J Lipid Res. 2013;54(5):1335–45.

Stadtman ER, Moskovitz J, Levine RL. Oxidation of methionine residues of proteins: biological consequences. Antioxidants & Redox Signaling. 2003;5(5):577–82.

Stadtman ER. Role of oxidant species in aging. Current Medicinal Chemistry. 2004;11(9):1105–12.

Stewart J, Slysz G, Pritting M, U M-E. Ferriheme and ferroheme are isosteric inhibitors of fatty acid binding to rat liver fatty acid binding protein. Biochem Cell Biol. 1996;74(2):249–55.

Stierlin H, Faigle J. Biotransformation of Diclofenac Sodium (Voltaren®) in Animals and in Man.: II. Quantitative determination of the unchanged drug and principal phenolic metabolites, in urine and bile. Xenobiotica. 1979;9(10):611–2.

Stirnimann G, Kessebohm K, Lauterburg B. Liver injury caused by drugs: an update. Swiss Medical Weekly. 2010;

Storch J, Thumser A. The fatty acid transport function of fatty acid-binding proteins. Biochimica Et Biophysica Acta Bba - Mol Cell Biology Lipids. 2000;1486(1):28–44.

Sumida Y, Niki E, Naito Y, Yoshikawa T. Involvement of free radicals and oxidative stress in NAFLD/NASH. Free Radical Res. 2013;47(11):869–80.

Sutti S, Jindal A, Locatelli I, Vacchiano M, Gigliotti L, Bozzola C, et al. Adaptive immune responses triggered by oxidative stress contribute to hepatic inflammation in NASH. Hepatology. 2014;59(3):886–97.

Sweetser D, Birkenmeier E, Klisak I, Zollman S, Sparkes R, Mohandas T, et al. The human and rodent intestinal fatty acid binding protein genes. A comparative analysis of their structure, expression, and linkage relationships. J Biol Chem. 1987;262(33):16060–71.

Szocs K. Endothelial dysfunction and reactive oxygen species production in ischemia/reperfusion and nitrate tolerance. Gen Physiol Biophys. 2004;23(3):265–95.

Takahashi K, Odani S, Ono T. A close structural relationship of rat liver Z-protein to cellular retinoid binding proteins and peripheral nerve myelin P2 protein. Biochem Biophys Res Commun. 1982;106(4):1099–105.

Tang W, Stearns R, Bandiera S, Zhang Y, Raab C, Braun M, et al. Studies on cytochrome P-450-mediated bioactivation of diclofenac in rats and in human hepatocytes: identification of glutathione conjugated metabolites. Drug Metab Dispos. 1999;27(3):365–72.

Teresa K-J, Ruta M, Wiśniewska K, Łankiewicz L, Dyba M. Products of Cu(II)-catalyzed oxidation in the presence of hydrogen peroxide of the 1–10, 1–16 fragments of human and mouse β-amyloid peptide. J Inorg Biochem. 2004;98(6):940–50.

Thomas J, Poland B, Honzatko R. Protein sulfhydryls and their role in the antioxidant function of protein S-thiolation. Arch Biochem Biophys. 1995;319(1):1–9.

Thompson J, Winter N, Terwey D, Bratt J, Banaszak L. The crystal structure of the liver fatty acid-binding protein. A complex with two bound oleates. The Journal of Biological Chemistry. 1997;272(11):7140–50.

Tian Y, Li H, Wang S, Yan J, Chen Z, Li Z, et al. Association of L-FABP T94A and MTP I128T polymorphisms with hyperlipidemia in Chinese subjects. Lipids. 2015;50(3):275–82.

Trehan A, Kiełbus M, Czapinski J, Stepulak A, Huhtaniemi I, Adolfo R-M. REPLACR-mutagenesis, a one-step method for site-directed mutagenesis by recombineering. Sci Reports. 2016;6(1):19121.

Veerkamp J, Paulussen R, Peeters R, Maatman R, Moerkerk H, Kuppevelt T. Detection, tissue distribution and (sub)cellular localization of fatty acid-binding protein types. Mol Cell Biochem. 1990;98(1-2):11–8.

Veerkamp J, Maatman R. Cytoplasmic fatty acid-binding proteins: their structure and genes. Prog Lipid Res. 1995;34(1):17–52.

Videla L. Oxidative stress signaling underlying liver disease and hepatoprotective mechanisms. World J Hepatology. 2009;1(1):72.

Vork M, Glatz J, Surtel D, Van der Vusse G. Release of fatty acid binding protein and lactate dehydrogenase from isolated rat heart during normoxia, low-flow ischemia, and reperfusion. Can J Physiol Pharmacol. 1993;71(12):952–8.

Wang G, Bonkovsky HL, de Lemos A, Burczynski FJ. Recent insights into the biological functions of liver fatty acid binding protein 1. Journal of Lipid Research. 2015;56(12):2238–47.

Wang G, Gong Y, Anderson J, Sun D, Minuk G, Roberts M, et al. Antioxidative function of L-FABP in L-FABP stably transfected Chang liver cells. Hepatology. 2005;42(4):871–9.

Wang G, Shen H, Rajaraman G, Roberts M, Gong Y, Jiang P, et al. Expression and antioxidant function of liver fatty acid binding protein in normal and bile-duct ligated rats. Eur J Pharmacol. 2007;560(1):61–8.

Wang Q, Rizk S, Bernard C, Lai M, Kam D, Storch J, et al. Protocols and pitfalls in obtaining fatty acid-binding proteins for biophysical studies of ligand-protein and protein-protein interactions. Biochem Biophysics Reports. 2017;10:318–24.

Wardman P. Fluorescent and luminescent probes for measurement of oxidative and nitrosative species in cells and tissues: progress, pitfalls, and prospects. Free Radic Biol Med. 2007;43(7):995–1022.

Warnakulasuriya S, Parkkila S, Nagao T, Preedy V, Pasanen M, Koivisto H, et al. Demonstration of ethanol-induced protein adducts in oral leukoplakia (pre-cancer) and cancer. J Oral Pathol Med. 2008;37(3):157–65.

Waugh D. An overview of enzymatic reagents for the removal of affinity tags. Protein Expres Purif. 2011;80(2):283–93.

Weber D, Davies M, Grune T. Determination of protein carbonyls in plasma, cell extracts, tissue homogenates, isolated proteins: Focus on sample preparation and derivatization conditions. Redox Biology. 2015;5:367–80.

Wei Y, Chen K, T W-C Adam, Stump CS, Ibdah JA, Sowers JR. Skeletal muscle insulin resistance: role of inflammatory cytokines and reactive oxygen species. American Journal of Physiology - Regulatory, Integrative and Comparative Physiology. 2008;294(3):R673–80.

Wolfrum C, Börchers T, Sacchettini J, Spener F. Binding of Fatty Acids and Peroxisome Proliferators to Orthologous Fatty Acid Binding Proteins from Human, Murine, and Bovine Liver†. Biochemistry-us. 2000;39(6):1469–74.

Wolfrum C, Borrmann CM, Börchers T, Spener F. Fatty acids and hypolipidemic drugs regulate peroxisome proliferator-activated receptors α- and γ-mediated gene expression via liver fatty acid binding protein: A signaling path to the nucleus. Proceedings of the National Academy of Sciences. 2001;98(5):2323–8.

Xu A, Wu L-J, Santella RM, Hei TK. Role of Oxyradicals in Mutagenicity and DNA Damage Induced by Crocidolite Asbestos in Mammalian Cells. Cancer Research. 1999;59(23):5922–6.

Yan J, Gong Y, She Y-M, Wang G, Roberts MS, Burczynski FJ. Molecular mechanism of recombinant liver fatty acid binding protein's antioxidant activity. Journal of Lipid Research. 2009;50(12):2445–54.

Young C, Britton Z, Robinson A. Recombinant protein expression and purification: A comprehensive review of affinity tags and microbial applications. Biotechnol J. 2012;7(5):620–34.

Zhang J, Stanley RA, Melton LD. Lipid peroxidation inhibition capacity assay for antioxidants based on liposomal membranes. Molecular Nutrition & Food Research. 2006;50(8):714–24.

Zhang L, Zhu X, Jiao D, Sun Y, Sun H. Efficient purification of His-tagged protein by superparamagnetic Fe3O4/Au–ANTA–Co2+ nanoparticles. Mater Sci Eng C. 2013;33(4):1989–92.